minerals

MDPI

Review

Chemical Composition Data of the Main Stages of Copper Production from Sulfide Minerals in Chile: A Review to Assist Circular Economy Studies

Kayo Santana Barros [1,*], Vicente Schaeffer Vielmo [1], Belén Garrido Moreno [1,2], Gabriel Riveros [3], Gerardo Cifuentes [2] and Andréa Moura Bernardes [1]

[1] Department of Materials Engineering, Federal University of Rio Grande do Sul (UFRGS), Avenue Bento Gonçalves, 9500, Porto Alegre 91501-970, Brazil; vicentevielmo@gmail.com (V.S.V.); belen.garridom@usach.cl (B.G.M.); amb@ufrgs.br (A.M.B.)
[2] Departamento de Ingeniería Metalúrgica, Facultad de Ingeniería, Universidad de Santiago de Chile, Avenida Libertador Bernardo O'Higgins 3363, Estación Central, Santiago 917022, Chile; gerardo.cifuentes@usach.cl
[3] Transducto S.A., Avenida La Dehesa 1201, Lo Barnechea, Santiago 917021, Chile; griveros@transducto.com
* Correspondence: kayobarros.s@gmail.com

Abstract: The mining industry has faced significant challenges to maintaining copper production technically, economically, and environmentally viable. Some of the major limitations that must be overcome in the coming years are the copper ore grade decline due to its intense exploitation, the increasing requirements for environmental protection, and the need to expand and construct new tailings dams. Furthermore, the risk of a supply crisis of critical metals, such as antimony and bismuth, has prompted efforts to increase their extraction from secondary resources in copper production. Therefore, improving conventional processes and developing new technologies is crucial to satisfying the world's metal demands, while respecting the policies of environmental organizations. Hence, it is essential that the chemical composition of each copper production stage is known for conducting these studies, which may be challenging due to the huge variability of concentration data concerning the ore extraction region, the process type, and the operational conditions. This paper presents a review of chemical composition data of the main stages of copper production from sulfide minerals, such as (1) copper minerals, (2) flotation tailings, (3) flotation concentrates, (4) slags and (5) flue dust from the smelting/converting stage, (6) copper anodes, (7) anode slimes, (8) contaminated electrolytes from the electrorefining stage, (9) electrolytes cleaned by ion-exchange resins, and (10) elution solutions from the resins. In addition, the main contributions of recent works on copper production are summarized herein. This study is focused on production sites from Chile since it is responsible for almost one-third of the world's copper production.

Keywords: Chilean copper production; Chuquicamata; tailings; copper electrorefining; antimony

Citation: Barros, K.S.; Vielmo, V.S.; Moreno, B.G.; Riveros, G.; Cifuentes, G.; Bernardes, A.M. Chemical Composition Data of the Main Stages of Copper Production from Sulfide Minerals in Chile: A Review to Assist Circular Economy Studies. *Minerals* **2022**, *12*, 250. https://doi.org/10.3390/min12020250

Academic Editors: Weiguo Xie, Hylke J. Glass and Eiman Amini

Received: 29 December 2021
Accepted: 11 February 2022
Published: 16 February 2022

1. Introduction

Copper is a metal that presents several industrial applications due to its attractive properties, such as electrical conductivity, thermal conductibility, and ductility. It is mainly used in electrical wiring, industrial machinery, plastic electroplating, printed wiring boards, zinc die casting, automotive bumpers, and rotogravure rolls [1,2]. Copper is especially important in the semiconductor industry because, in general, the connections on chips are made of this metal due to its low electrical resistance, good mechanical properties, and high corrosion resistance [3]. In addition to this, copper can form alloys with various elements.

Copper is found in nature mainly in the form of sulfide and oxide minerals, and the main copper mines are present in Chile, Australia, Peru, China, the USA, and Mexico [4]. In Chile, the world's largest copper producer, most of the copper is obtained from sulfide

ores [5,6]. Since copper sulfide ores present impurities, several purification steps are carried out to obtain a high-purity copper product. Figure 1 shows a simplified representation of copper production from sulfide minerals. Note that the ore is submitted basically to comminution, concentration, casting, and electrorefining stages [7,8].

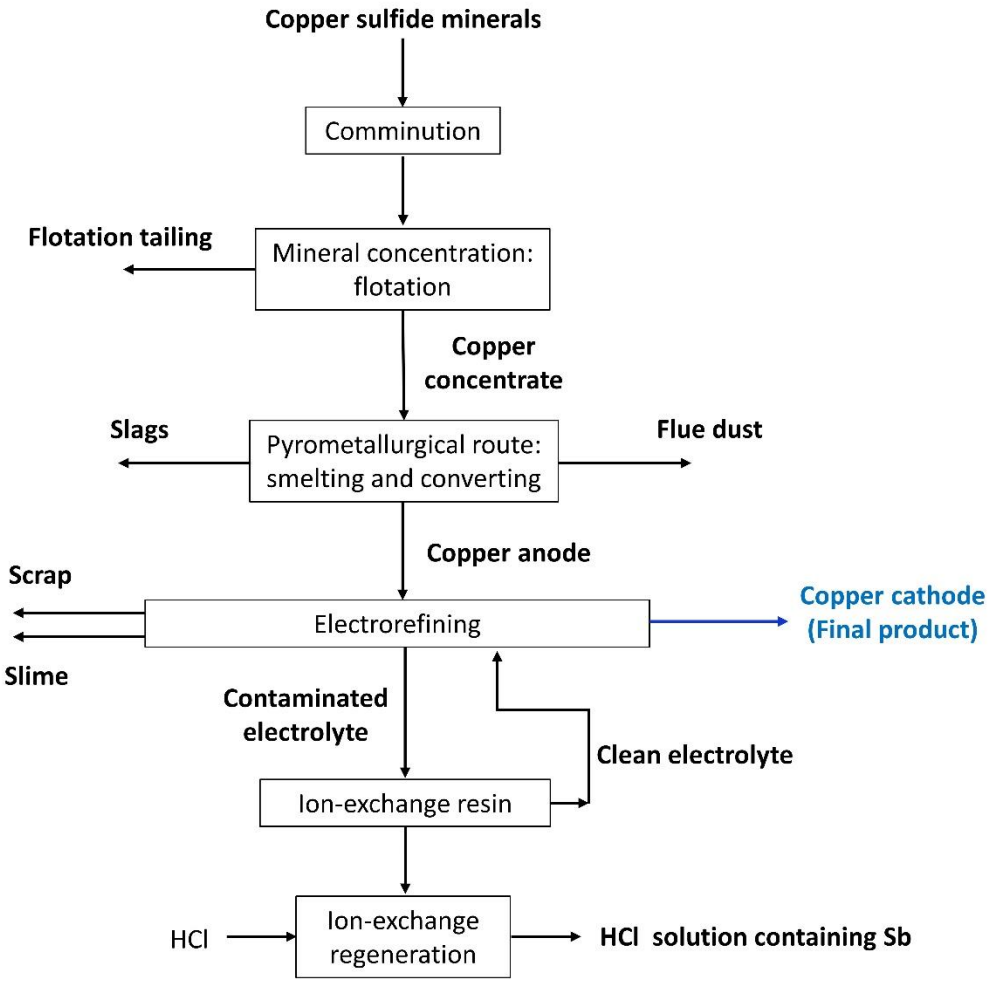

Figure 1. Flowchart of the copper production from sulfide minerals showing the inputs and outputs of the main process stages.

The comminution stage aims to reduce the ore particle size through crushing, grinding, or other processes, being an energy-intensive operation with very low efficiency; it is estimated that comminution accounts for 30%–50% of typical mining operating costs [9,10]. This is expected to intensify in the coming years due to the lower ore grades, the increase in rock hardness, and the depth of the mines. Therefore, researchers have been evaluating methods to reduce the energy consumption in the comminution process of copper ores [9,11–13].

The copper concentration stage is usually conducted via flotation to separate the valuable minerals from the gangue material. The most important factors that affect the flotation performance are the ore characteristics, such as its mineral structure and the surface properties of the particle, the mechanical parameters of the cell, and the operating conditions, such as the solution pH [14,15]. One of the major concerns regarding flotation is the generation of tailings, which is the waste material that may still contain copper and other valuable metals. It is expected that the tailings production will increase in the coming years due to the intense extraction of low-grade copper ores [16]. This may limit the copper production in Chile due to the scarcity of areas available to expand tailings

dams or construct new ones [5]. Hence, authors have been evaluating methods to improve flotation processes, reduce and reprocess fresh and old tailings [17–21].

The pyrometallurgical route involves smelting, converting and fire refining steps, which aim to separate the metal from its minerals and obtain copper anode. In the smelting stage, the concentrated flotation product (copper concentrate) is converted to molten high-Cu sulfide matte at temperatures of 1200–1300 °C [7]. In the converting stage, air is injected into the liquid phase, which is composed basically of copper and iron sulfides; the iron sulfide is oxidized and the copper sulfide is converted into crude molten copper (~99%) [22]. In the fire refining stage, the remaining sulfur and oxygen in the blister copper are eliminated through oxidation; sulfur is removed by adding O_2 (air), which reacts with S to form SO_2, whereas CO and H_2 are added to reduce Cu_2O and form Cu, CO_2 and H_2O [7]. Thus, the fire-refined copper complies with the chemical specifications to be electro-refined. In these processes, large amounts of waste are generated, especially flue dust and slags [23]. As flue dust contains copper with several impurities, such as As, Sb, Bi, Pb, and Cd, it cannot be returned directly to the smelting furnace since this would increase the content of impurities in the feed material and decrease the furnace processing capability [24,25]. The formation of huge amounts of slags generates technical and environmental problems since they are deposited at landfills [26]. Therefore, researchers have been evaluating the minimization of dust and slag formation, the recovery of copper, and the extraction of valuable metals from these waste materials [22,27–29].

Lastly, the electrorefining stage aims at purifying the copper anode to generate the final copper product as a cathode. One of the major challenges in this process is controlling the concentration of metals in the tankhouse electrolyte that dissolve from the anode along with copper, such as arsenic, antimony, and bismuth. In general, the molar ratio of As/(Sb+Bi) is controlled and kept in a suitable range where Sb and Bi produce a minor effect. However, this increases health problems and the impurities are lost in the anode slime [30,31]. Antimony and bismuth are valuable metals widely used in semiconductor, thermoelectric, pharmaceuticals, chemicals, ceramics, and pigments, also being considered as critical elements by the European Commission [32,33]. Thus, extracting and recovering these metals from copper production has become increasingly important. In recent years, several methods have been tested for removing these impurities from tankhouse electrolytes, such as chemical precipitation [34,35], solvent extraction [36,37], using activated carbon [38,39], chemical leaching [40], electrodialysis [41], electrowinning [32], and ion-exchange resins [30,42]. Among these technologies, ion-exchange resins are used on industrial scale worldwide [30].

In the coming years, the mining industry will face a challenging scenario due to the gradual reduction in the mineral resources' purity, while the global demand for copper and the stringency of environmental policies tend to increase considerably. The reduction in copper ore grade that occurred in the recent years and the projection for the coming years in Australia, Peru, Chile, Indonesia, Mexico, and USA may be seen in Figure 2 [43]. This is particularly challenging for Chile since mining is the most important economic activity in the country [44]. Lagos et al. [5] have recently projected that, from 2030, copper production in Chile will decrease due to the lack of technologies that would make the extraction of low-grade ores feasible. This can be seen in Figure 3, which shows the projection of copper production from oxide (blue line) and sulfide (red line—concentrates) ores obtained by Lagos et al. [5] considering economic, regulatory, and environmental constraints. Similar trends were reported by Northey et al. [45], who presented scenarios for copper production worldwide until 2150 based on a detailed assessment of global copper resources and historic mine production. The results for historic and modelled copper production by selected countries are shown in Figure 4. Note that, by 2040, all countries will experience a strong reduction in their production, and this will be more critical for Chile because this country will be the largest copper producer before the decline in its production.

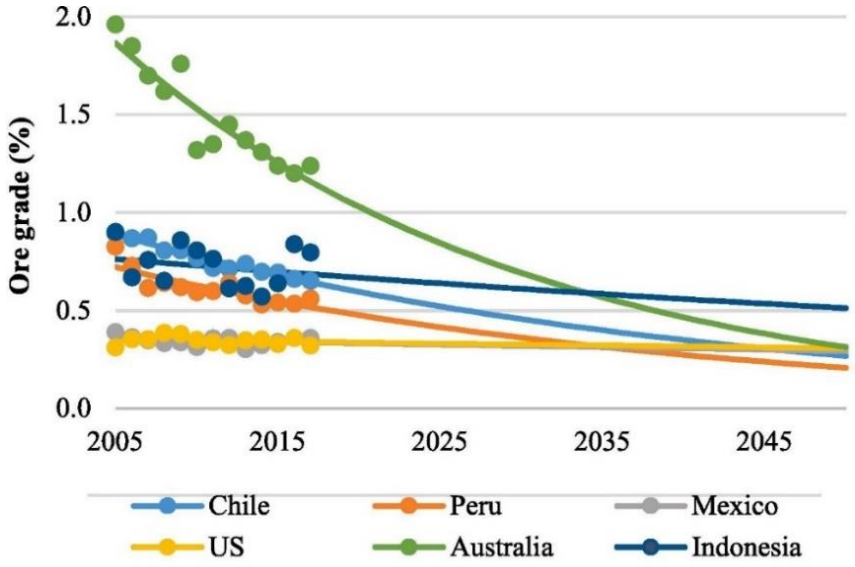

Figure 2. Reported (symbols) and forecasted (lines) ore grade by country (Adapted from [43] with permission).

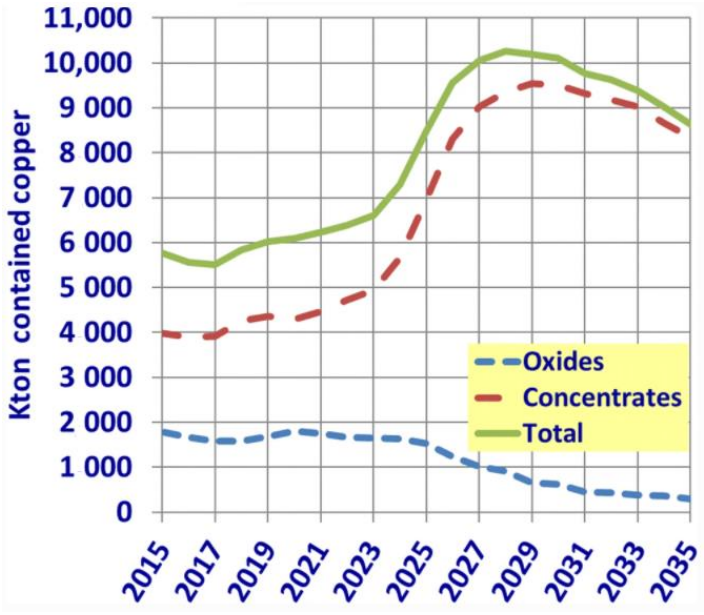

Figure 3. Projection of copper production in Chile in the coming years from oxide and sulfide (concentrate) ores (Adapted from [5] with permission).

Several studies have been carried out to improve Chilean copper production, reducing operational costs, reprocessing tailings, reducing losses of valuable metals, and making the processes safer for the environment and human health [8,20,22,28,46–52]. For the development of these studies, knowing the chemical composition of each processing stage is essential; one of the limitations in the studies on copper production is the huge variability of concentration data depending on the region where copper is obtained, the process type, and the operational conditions. Thus, the knowledge of the chemical composition of each production stage may encourage the development of technologies to improve copper production and recover products from wastes, assisting the industrial supply of resources to feed the circular economy.

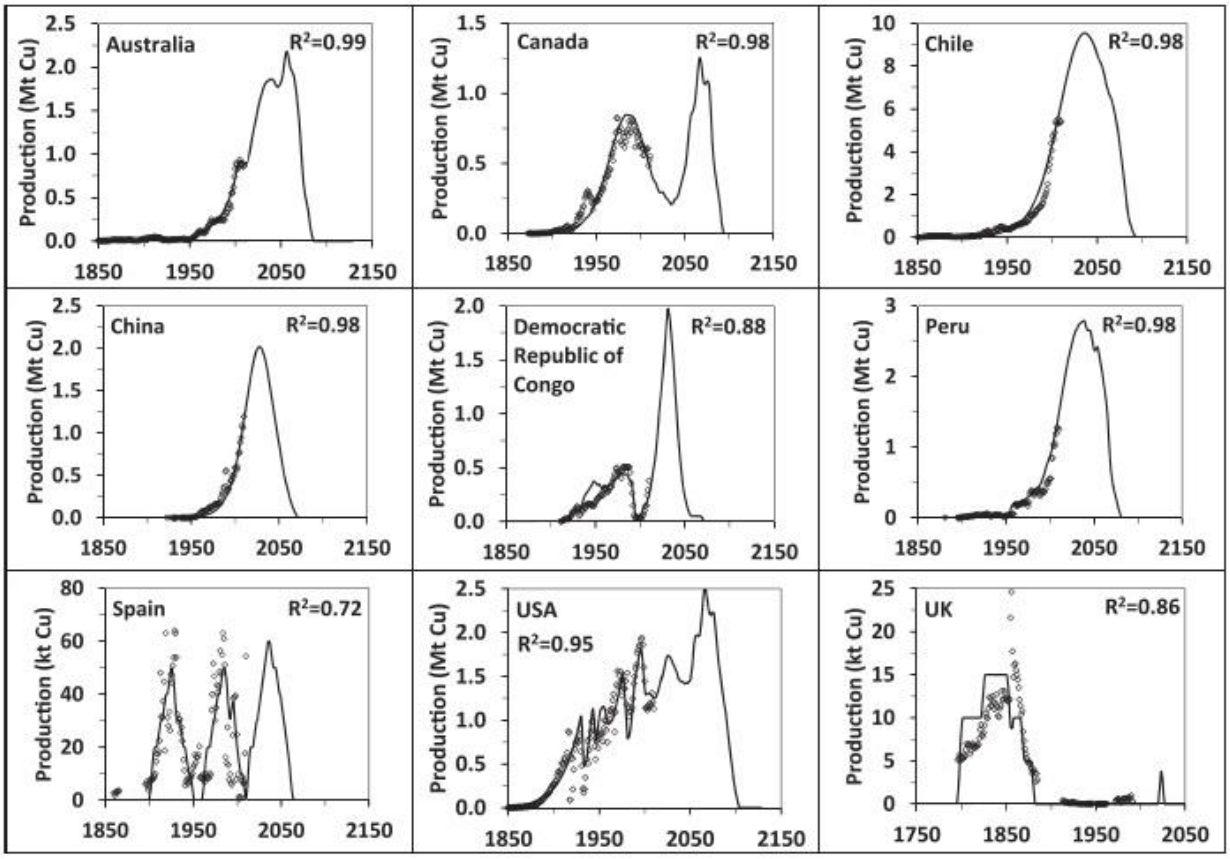

Figure 4. Historic copper production data (symbols) and modelled (line) scenarios for selected countries [45].

The present work provides a review of the copper production from sulfide minerals focused on the concentration data of the main stages of the process (shown in Figure 1) and the recent advances in the development of technologies for copper mining. The data shown herein are focused on production sites from Chile since this country is responsible for almost one-third of the world's copper production. The main objective of this review is to assist future works on optimization of copper production in Chile, making the processes economically and environmentally viable, and allowing the recovery of valuable and critical metals from secondary resources, which will strengthen the circular economy.

2. Copper Sulfide Minerals

Copper is found in nature mainly in oxide and sulfide ores. The oxide ores are processed via hydrometallurgical routes because they are easily dissolved in acid. Conversely, sulfide ores are practically insoluble in acid and must undergo pyrometallurgical routes [40]. Table 1 shows the main copper minerals found in nature [40,53–55].

About 80% of the world's copper production comes from sulfide minerals, but their composition varies considerably depending on the region where the ore is obtained [56]. Table 2A shows the mineralogical composition of copper sulfide ores from different Chilean regions. Note that the main copper mineral from Lomas Bayas, El Salvador, and Escondida mines is chalcocite (15.3%, 21% and 53%, respectively), whereas the main copper mineral from Chuquicamata mine, one of the largest copper producers in the world, is covellite (17%). The copper ores from El Teniente and Andina mines are mainly composed of chalcopyrite (86%–90% and 81%, respectively) [57,58]. It is worth highlighting the presence of molybdenite in Chilean minerals, such as in El Salvador, Andina and Escondida mines, making Chile one of the world's major producers of molybdenum [59]. A recent and detailed characterization of copper sulfide ores from Antofagasta region, Chile, is shown in Table 2B.

Note that pyrite accounts for 0.68% of the mineral, whereas chalcocite/digenite/covellite account for 0.42% and chalcopyrite/bornite 0.08%. Data on the mineralogical composition of copper oxide ores from Chile may be found elsewhere [60].

Table 1. Main copper minerals found in nature.

Type	Mineral	Formula
Oxides	Cuprite	Cu_2O
	Tenorite	CuO
	Malachite	$CuCO_3{\cdot}Cu(OH)_2$
	Azurite	$(CuCO_3)_2{\cdot}Cu(OH)_2$
	Chrysocolla	$CuO{\cdot}SiO_2{\cdot}2H_2O$
	Atacamite	$Cu_2Cl(OH)_3$
Sulfides	Chalcocite	Cu_2S
	Covellite	CuS
	Chalcopyrite	$CuFeS_2$
	Bornite	Cu_5FeS_4
	Stannite	Cu_2FeSnS_4
	Enargite	Cu_3AsS_4
	Tennantite	$Cu_{12}As_4S_{13}$
	Famatinite	Cu_3SbS_4
	Tetrahedrite	$Cu_{12}Sb_4S_{13}$

Table 2. Mineralogical composition of copper ore samples from Chile (wt%).

A							
Ref.	[51]	[61]	[61]	[61]	[61]	[57]	[62]
Mine	**Lomas Bayas**	**El Salvador**	**Chuquicamata**	**Andina**	**Escondida**	**El Teniente**	**Unknown**
Pyrite	55.9	38	35	6.2	30		
Chalcocite	15.3	21	11.2	1.5	53		5.92
Bornite	11.3	1.51	1.65	0.27	0.11	6–9	18.85
Covellite	7.9	14	17	1.1	0.6		0.71
Chalcopyrite	7.7	7.5	12	81	4.8	86–90	74.51
Digenite	0.6						
Enargite		2.1	5.3	0.6	0.36		0.01
Molybdenite		0.29		0.89	0.29		
Metallic copper				0.46	0.16		
Cuprite					0.5		
Hematite				0.2	0.08		
Others	1.3	15.44	17.7	7.9	10.07		
B							
Antofagasta Region							
Ref. [63]							
Pyrite	0.68	Magnetite	0.11	Kaolinite Group	1.88		
Chalcocite/Digenite/Covellite	0.42	Goethite	0.01	Muscovite/Sericite	0.74		
Chalcopyrite/ Bornite	0.08	Other Cu Minerals	0.38	Chlorite/Biotite	10.87		
Enargite/Tennantite/Tetrahedrite	0	Other Fe Oxides/Sulfates	0.26	Other Phyllosilicates	0.92		
Native Cu/Cuprite/Tenorite	0	Quartz	24.44	Others	0.53		
Molybdenite	0.01	Feldspars	58.66				

The chemical composition of Chilean copper sulfide ores in terms of Cu and Fe concentrations are shown in Table 3A, whereas Table 3B shows a more detailed chemical composition of copper sulfide ores from northern Chile. Note that the copper concentration varies between approximately 0.7 and 2.1 wt% depending on the region. Concentration data for other elements in copper ores, such as the critical metals, are scarce in the literature due to the difficulty in determining the composition of trace elements. Data on the chemical composition of oxide copper ores from Chile may also be found in the literature [60].

Table 3. Chemical composition of copper sulfide ores from Chile (wt%).

A		Chemical Composition (wt%)	
Ref.	**Mine/region**	**Cu**	**Fe**
[64]	Northern Chile	1.49	10.36
[65]	Cerro Colorado	1.28–2.05	1.47–1.99
[57]	El Teniente	1.20	
[7]	Los Bronces	1.06	
[7]	Candelaria	0.9–1.0	
[66]	Unknown	0.7–0.86	

B		Chemical Composition (wt%)											
Ref.	**Mine/region**	**Cu**	**Fe**	**SiO_2**	**Al_2O_3**	**As**	**Pb**	**Zn**	**Ag**	**S**	**CaO**	**Mg**	**Au**
[64]	Northern Chile	1.49	10.36	48.09	8.6	<0.1	0.049	0.037	<5	2.26	8.07	2.92	<0.2

3. Mineral Processing: Comminution

The first stage of copper processing is the comminution, which is carried out to liberate the copper-bearing minerals from the gangue by reducing the ore particle size. Firstly, explosions are made in the mine to crack the rocks, generating various fragments of ore. Then, these large fragments are compressed in crushers, which is also generally done in the mine. Lastly, water is added to the crushed ore and this mixture is forwarded to grinding mills, where the ore particle size is further reduced, and the copper minerals are liberated [7]. The comminution process is energy-intensive, the energy consumption being strongly dependent on the composition and texture of the ore, such as the mineral grain size distribution and mineral association [59,67].

4. Mineral Concentration: Flotation

4.1. Copper Concentrate

After being subjected to the comminution step, the minerals proceed to the concentration step via flotation, filtration, and drying. Flotation aims at the selective separation and recovery of copper-bearing minerals. Thus, it generates a process stream concentrated in copper, which is subsequently forwarded to the smelting and converting stages, and another stream of flotation tailings. The flotation technique allows concentration of copper sulfide minerals by exploiting differences in their surface properties, by adding chemical reagents able to make copper sulfide minerals hydrophobic [68,69]. Then, air is injected at the bottom of the flotation cell to promote the migration of hydrophobic copper sulfide minerals to the surface. Lastly, this copper-rich material is dewatered, achieving a copper concentration of 20%–45% [69].

The efficiency of a flotation operation depends on the nature and texture of the particles (such as mineralogy, morphology, particle size, mineral association) as well as the type and design of flotation cells and operating variables (such as pH, air flowrate, pulp density, reagent type and dosage). Therefore, several authors have investigated methods to increase the efficiency of flotation processes [21,64,70–74]. In particular, the influence of particle size on flotation has been frequently evaluated since fine and coarse particles follow different trends in flotation, affecting the process efficiency considerably [21,65]. In general, the maximum recovery of copper from sulfide ores is achieved at the intermediate particle size range of 50–70 μm [75].

Another factor that must be evaluated to guarantee the efficiency of flotation is the mineral composition. In copper flotation, non-valuable iron sulfides (mostly pyrite) are often associated with valuable sulfide minerals, such as chalcocite and chalcopyrite. Thus, the separation of pyrite from copper minerals is crucial in the flotation stage [14,76].

Figure 5 shows the mineralogical composition of several flotation concentrates from the world's leading copper producers, including the Chilean ones [77]. Note that they are mostly composed of chalcopyrite, chalcocite, and pyrite. In Chuquicamata mine, the frac-

tion of covellite is also high. These results differ from those reported by Fuentes et al. [52], who reported the mineralogical composition of two flotation concentrate samples from Chuquicamata; the results obtained by Fuentes et al. are shown in Table 4. According to the authors, digenite is the main mineral containing copper in both samples, followed by chalcopyrite and covellite. These results showed by Fuentes et al. [52] agree with those presented in another work of the authors [49]; it was reported that the main mineral components in the flotation concentrates from Chuquicamata are digenite, pyrite, chalcopyrite, bornite, covellite, and sphalerite, with minor amounts of enargite, galena, and molybdenite. This difference between the data reported by the authors can be explained by the change in the mineralogy of the ore as the exploitation of Chuquicamata has intensified, since the data reported by Flores et al. [77] are recent (2020), whereas those reported by Fuentes et al. [52] are from 2009.

Table 5 presents the chemical composition of copper concentrates obtained in different regions and companies from Chile.

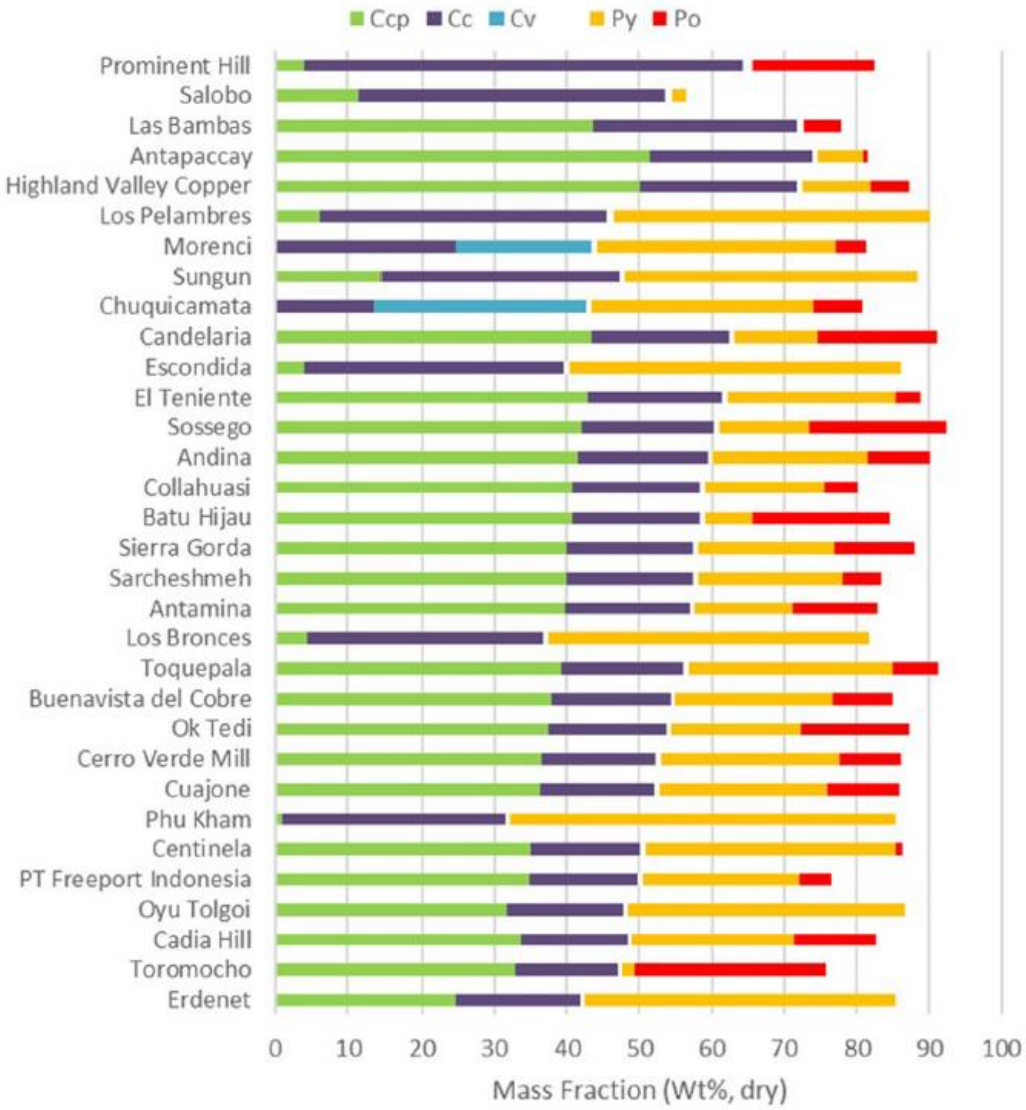

Figure 5. Mineralogical composition of copper concentrates from the world's leading copper producers. Ccp, Cc, Cv, Py, and Po are chalcopyrite, chalcocite, covellite, pyrite, and pyrrhotite, respectively [77].

Table 4. Mineralogical composition of concentrates from Chuquicamata mine (% v/v, relative to the total sulfide phase) [52].

Mineral	Sample 1 (% v/v)	Sample 2 (% v/v)
Digenite	34	26
Pyrite	24	35
Chalcopyrite	23	21
Covellite	9	9
Bornite	6	3
Sphalerite	3	4
Enargite	1	2
Molybdenite	~0.1	~0.1
Galena	~0.1	~0.1

Table 5. Chemical composition (wt%) of Chilean copper concentrates.

Ref.	[52]	[52]	[27]	[28]	[7]
Mine/Region		**Chuquicamata**		**Unknown**	**Potrerillos**
Cu	33.5	31.8	36.1	36.1	30
Fe	21.6	18.3	22.9	22.9	25
S	33.4	31.8	32.6	32.6	32
Pb	0.090	0.091	0.20	0.20	
Zn	2.10	3.07	0.70	0.70	
Bi	0.0069	0.011	0.1	0.05	
Sb	0.012	0.042	0.01	0.01	
As	0.48	0.79	0.7	0.7	
Hg	0.0021	0.00069			
Mo	0.16	0.055			
Te	0.00047	0.001			
Tl	0.00004	0.00011			
Cd	0.0103	0.0110			
SiO_2	5.4	8.0			4

According to Table 5, in Chuquicamata mine, the concentrate contains ~33 wt% of Cu and several other species, mainly Fe, S, Si, Zn, As, Pb, Mo, and Sb. Concentrates from Potrerillos mine possess a Cu concentration of 30 wt%, whereas the concentration data of other elements are scarce in the literature.

4.2. Flotation Tailings

Flotation tailings are stored in dams located near the mine. Water is reclaimed from these dams and recycled to the concentrator. In some regions of Chile, such as the northern region, water is scarce. Therefore, some mining companies use seawater in the flotation operation, such as the Las Luces mine, owned by the Las Cenizas Mining Group [78]. A recent review showed that the use of seawater in the Chilean mining industry will increase in the coming years due to the depletion of other water resources and because the mineral concentration step requires large volumes of water [79]. The seawater can be directly used in mining or can undergo a desalination step. The first case does not involve the costs and impacts of the demineralization process, but the presence of chloride ions is challenging due to equipment corrosion. In the second case, additional operational costs are involved due to electricity consumption, besides the environmental impacts. Therefore, new demineralization technologies are expected to be developed in the coming years for application in the mining industry.

One of the biggest challenges that Chilean mining companies have faced is the generation and disposal of tailings. According to the report released in 2020 by SERNAGEOMIN (Servicio Nacional de Geología y Minería de Chile), most of the flotation tailings dam in Chile are inactive or abandoned [80]. It is estimated that by 2035 the generation of tailings

per year will be 3.25 times greater than the amount generated in 2015 [5]. This causes huge concerns due to the scarcity of areas available, besides the social and environmental risks involved [18]. In 1965, an earthquake caused the disruption of a tailings dam in El Cobre (Chile), which killed approximately 200 people [81]. In 2015 and 2019, two other tragedies involving tailings dams occurred in the region of Minas Gerais, Brazil, which culminated in deaths and significant destruction of the environment. These events in Brazil increased the social and regulatory resistance to the construction of tailings dams in Chile [5]. Figure 6 shows the number of accidents involving tailings dam failures in several countries from 1910 to 2018 [81]; note that Chile is responsible for the second largest number.

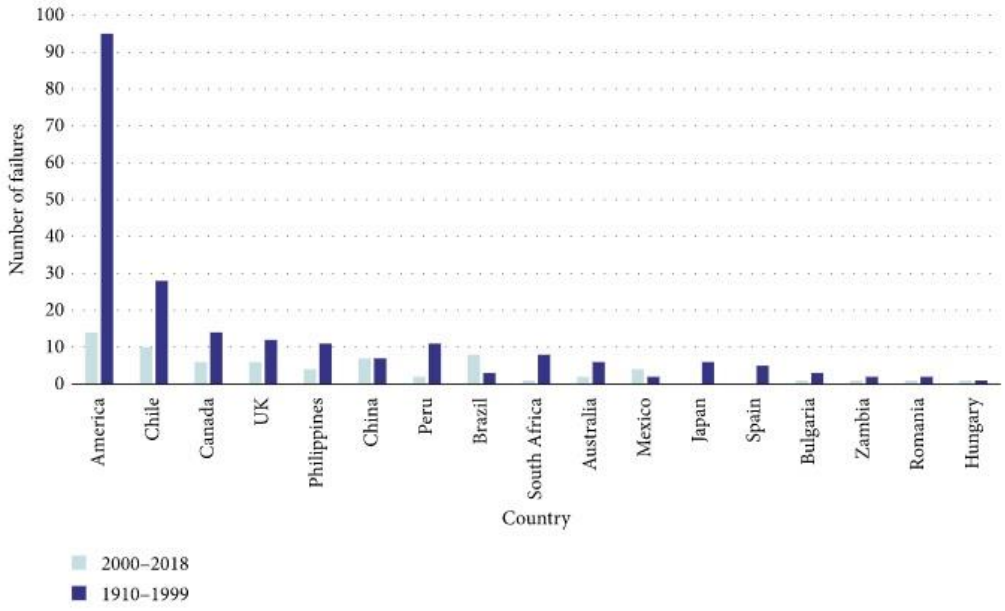

Figure 6. Number of accidents involving tailings dam failures in several countries from 1910 to 2018 [81].

Another problem regarding flotation tailings dams is the occurrence of acid mine drainage due to the oxidation of liberated sulfide minerals, which may cause severe detrimental effects on underground and surface water bodies [82]. This occurrence is often due to the presence of chalcocite, chalcopyrite, and mainly pyrite in the tailings. In Chile, the pyrite content in tailings varies between 4% and 8% [18].

A tertiary issue may arise whilst reprocessing the flotation tailings, as is observed in Codelco Salvador (Chile), where a secondary flotation tailings stream presenting high levels of SiO_2 and Al_2O_3 and lower copper content is generated, which hinders its further processing [83].

In light of the above-mentioned concerns, in recent years, several authors have evaluated the reprocessing of fresh and old tailings from the mining industry in Chile [17,44,48,50,84,85]. Recently, authors have also investigated the use of Chilean copper-treated tailings as supplementary cementitious materials to improve properties of concrete [86,87], the use of copper tailings deposits for the sequestration of CO_2 [88], and the re-processing of tailings to obtain critical raw materials [89,90]. Considering the importance of determining the chemical composition of tailings to reduce their generation or to reprocess it, Table 6A,B present composition data of flotation tailings from several Chilean regions. The data presented in Table 6B, which were recently reported by Araya et al. [89], show the concentration of several valuable and critical metals in flotation tailings from five Chilean regions (Sierra Gorda, Mantos Blancos, Talabre, Esperanza and Laguna Seca). Data on the composition and mineralogical characterization of porphyry copper tailings from Chilean mines may also be found in Refs. [85,87].

Table 6. Chemical composition of Chilean flotation tailings from copper production.

	A (wt%)								
Ref.	[91]	[44]	[92]	[64]	[50]	[93]	[18]	[94]	[7]
Mine/ Region	**El Teniente**	**Northern Chile, Atacama Desert**	**Northern Chile, Atacama Desert**	**Northern Chile**	**Commune of Taltal, Antofagasta Region**	**Commune of Taltal, Antofagasta Region**	**Atacama Desert**	**Las Tórtolas, Central Chile**	**El Soldado/Los Bronces/Mantos Blancos**
Cu	1.05	1.115	1.0571	0.050	0.1527	0.1315–0.6566	0.260	0.0485	0.180/0.133/0.120 (respectively)
Fe	41.78	3.5015	3.5488	9.86	7.20		16.12		
SiO_2	40.5			54.2					
Al_2O_3				10.13					
Al			2.3841		8.30				
Pb		0.01832	0.007565	0.034		0.0015–0.02041			
Ni						0.0017–0.0085			
Zn		0.02822	0.02967	0.047	0.0221	0.0167–0.0381		0.0041	
S				0.03			2.71		
SO_4^{2-}		0.21982	0.33826						
Au				0.1		0.00001–0.00005			
Ag				<5					
CaO				6.54					
Ca		0.02925	0.02797		2.9				
MgO				3.74					
As			0.000363	<0.01		0.00155–0.00306			
Mg			0.01066		2.3				
K			0.001804		4.1				
Na		0.3265	0.32701		1.5				
Cr			0.000289						
Ti					0.4				
Mo			0.01337					0.0109	
Mn		0.03525	0.03228		0.1379	0.0952–0.1631			
Sr					0.0219				
P					0.1384				
Cl			0.8774						
Ba					0.069				
Cd			0.000134					<0.000002	
B			0.00641						
Ce					0.0234				
Hg						0.00006–0.0011			

Table 6. *Cont.*

A (wt%)												
Ref.	[91]	[44]		[92]	[64]	[50]	[93]	[18]	[94]		[7]	
Mine/ Region	**El Teniente**	**Northern Chile, Atacama Desert**		**Northern Chile, Atacama Desert**	**Northern Chile**	**Commune of Taltal, Antofagasta Region**	**Commune of Taltal, Antofagasta Region**	**Atacama Desert**	**Las Tórtolas, Central Chile**		**El Soldado/Los Bronces/Mantos Blancos**	
Mine/Region	**B (g/t and wt%) [89]**											
Sierra Gorda	Cu (g/t)	V (g/t)	Co (g/t)	Y (g/t)	Nb (g/t)	Ba (g/t)	Sc (g/t)	Hf (g/t)	Ta (g/t)	Sb (g/t)	Bi (g/t)	Ni (g/t)
	981	125	12	82	28	486	11	8.56	0.13	10.31	<10	84
	Zn (g/t)	Rb (g/t)	Sr (g/t)	Zr (g/t)	Pb (g/t)	Cs (g/t)	Th (g/t)	U (g/t)	As (g/t)	Mo (g/t)	Sn (g/t)	Ag (g/t)
	159	329	68	557	50	6.53	55.93	22.23	<20	415.97	85.2	21.4
	Cd (g/t)	W (g/t)	La (g/t)	Ce (g/t)	Pr (g/t)	Nd (g/t)	Sm (g/t)	Eu (g/t)	Gd (g/t)	Tb (g/t)	Dy (g/t)	Ho (g/t)
	12.1	<10	42.71	80.38	10.15	34.12	7.55	1.01	6.07	0.85	4.47	0.87
	Er (g/t)	Tm (g/t)	Yb (g/t)	Lu (g/t)	Au (g/t)	Hg (g/t)	Cr (g/t)	S Total (%)	SiO_2 (%)	Al_2O_3 (%)	TiO_2 (%)	Fe_2O_3 (%)
	2.41	0.36	2.35	0.32	<0.02	0.03	41	0.85	63.09	14.43	0.55	5.91
	CaO (%)	MgO (%)	MnO (%)	Na_2O (%)	K_2O (%)	P_2O_5 (%)	PPC (%)	SO_3 (%)				
	0.8	2.05	0.09	1.58	6.01	0.13	4.74	-				
Mantos Blancos	Cu (g/t)	V (g/t)	Co (g/t)	Y (g/t)	Nb (g/t)	Ba (g/t)	Sc (g/t)	Hf (g/t)	Ta (g/t)	Sb (g/t)	Bi (g/t)	Ni (g/t)
	1932	120	10.33	70	43	<20	16.33	6.303	<0.01	<10	<10	83.33
	Zn (g/t)	Rb (g/t)	Sr (g/t)	Zr (g/t)	Pb (g/t)	Cs (g/t)	Th (g/t)	U (g/t)	As (g/t)	Mo (g/t)	Sn (g/t)	Ag (g/t)
	72	29	108	347	140	1.9	14.11	4.867	<20	<5	106	25.8
	Cd (g/t)	W (g/t)	La (g/t)	Ce (g/t)	Pr (g/t)	Nd (g/t)	Sm (g/t)	Eu (g/t)	Gd (g/t)	Tb (g/t)	Dy (g/t)	Ho (g/t)
	11.2	<10	24.063	60.057	8.07	30.48	7.11	1.33	6.367	0.883	5.22	1.027
	Er (g/t)	Tm (g/t)	Yb (g/t)	Lu (g/t)	Au (g/t)	Hg (g/t)	Cr (g/t)	S Total (%)	SiO_2 (%)	Al_2O_3 (%)	TiO_2 (%)	Fe_2O_3 (%)
	2.99	0.42	2.83	0.387	<0.02	0.02	48.33	0.257	64.72	13.79	0.5	4.38
	CaO (%)	MgO (%)	MnO (%)	Na_2O (%)	K_2O (%)	P_2O_5 (%)	PPC (%)	SO_3 (%)				
	2.037	2.26	0.06	7.36	0.543	0.153	3.47	-				

Table 6. *Cont.*

A (wt%)												
Ref.	[91]	[44]		[92]	[64]	[50]	[93]	[18]	[94]		[7]	
Mine/ Region	**El Teniente**	**Northern Chile, Atacama Desert**		**Northern Chile, Atacama Desert**	**Northern Chile**	**Commune of Taltal, Antofagasta Region**	**Commune of Taltal, Antofagasta Region**	**Atacama Desert**	**Las Tórtolas, Central Chile**		**El Soldado/Los Bronces/Mantos Blancos**	
Mine/Region	**B (g/t and wt%) [89]**											
Talabre	Cu (g/t)	V (g/t)	Co (g/t)	Y (g/t)	Nb (g/t)	Ba (g/t)	Sc (g/t)	Hf (g/t)	Ta (g/t)	Sb (g/t)	Bi (g/t)	Ni (g/t)
	2296	70	6	62	39	518	22	6.3	<0.01	55.33	<10	77
	Zn (g/t)	Rb (g/t)	Sr (g/t)	Zr (g/t)	Pb (g/t)	Cs (g/t)	Th (g/t)	U (g/t)	As (g/t)	Mo (g/t)	Sn (g/t)	Ag (g/t)
	231	124	498	568	741	0.89	1.74	1.67	783	124.39	46.7	17.9
	Cd (g/t)	W (g/t)	La (g/t)	Ce (g/t)	Pr (g/t)	Nd (g/t)	Sm (g/t)	Eu (g/t)	Gd (g/t)	Tb (g/t)	Dy (g/t)	Ho (g/t)
	3.29	88.8	6.98	11.88	1.44	5.54	1.02	0.4	0.86	0.11	0.6	0.12
	Er (g/t)	Tm (g/t)	Yb (g/t)	Lu (g/t)	Au (g/t)	Hg (g/t)	Cr (g/t)	S Total (%)	SiO_2 (%)	Al_2O_3 (%)	TiO_2 (%)	Fe_2O_3 (%)
	0.33	0.05	0.34	0.05	<0.02	0.5	19	0.96	67.81	14.34	0.18	2.06
	CaO (%)	MgO (%)	MnO (%)	Na_2O (%)	K_2O (%)	P_2O_5 (%)	PPC (%)	SO_3 (%)				
	1.89	0.38	0.03	1.06	4.09	0.08	4.79	2.4				
Esperanza	Cu (g/t)	V (g/t)	Co (g/t)	Y (g/t)	Nb (g/t)	Ba (g/t)	Sc (g/t)	Hf (g/t)	Ta (g/t)	Sb (g/t)	Bi (g/t)	Ni (g/t)
	675	160	11	49	21	185	26	3.88	<0.01	<10	<10	70
	Zn (g/t)	Rb (g/t)	Sr (g/t)	Zr (g/t)	Pb (g/t)	Cs (g/t)	Th (g/t)	U (g/t)	As (g/t)	Mo (g/t)	Sn (g/t)	Ag (g/t)
	83	99	295	313	20	1.71	4.28	1.44	<20	16.94	60.93	25.5
	Cd (g/t)	W (g/t)	La (g/t)	Ce (g/t)	Pr (g/t)	Nd (g/t)	Sm (g/t)	Eu (g/t)	Gd (g/t)	Tb (g/t)	Dy (g/t)	Ho (g/t)
	<1	<10	15.96	32.32	4.31	17.46	3.65	1.06	3.43	0.49	2.87	0.55
	Er (g/t)	Tm (g/t)	Yb (g/t)	Lu (g/t)	Au (g/t)	Hg (g/t)	Cr (g/t)	S Total (%)	SiO_2 (%)	Al_2O_3 (%)	TiO_2 (%)	Fe_2O_3 (%)
	1.71	0.26	1.6	0.23	<0.02	0.24	29	2.58	48.06	13.50	0.62	5.86
	CaO (%)	MgO (%)	MnO (%)	Na_2O (%)	K_2O (%)	P_2O_5 (%)	PPC (%)	SO_3 (%)				
	3.41	0.07	0.07	3.73	2.79	0.16	9.66	6.45				

Table 6. *Cont.*

A (wt%)												
Ref.	[91]	[44]		[92]	[64]	[50]	[93]	[18]	[94]		[7]	
Mine/ Region	**El Teniente**	**Northern Chile, Atacama Desert**		**Northern Chile, Atacama Desert**	**Northern Chile**	**Commune of Taltal, Antofagasta Region**	**Commune of Taltal, Antofagasta Region**	**Atacama Desert**	**Las Tórtolas, Central Chile**		**El Soldado/Los Bronces/Mantos Blancos**	
Mine/Region	**B (g/t and wt%) [89]**											
Laguna Seca	Cu (g/t)	V (g/t)	Co (g/t)	Y (g/t)	Nb (g/t)	Ba (g/t)	Sc (g/t)	Hf (g/t)	Ta (g/t)	Sb (g/t)	Bi (g/t)	Ni (g/t)
	1335	96.67	30.67	45	10.33	508	18.667	3.463	0.29	26.33	<10	16.33
	Zn (g/t)	Rb (g/t)	Sr (g/t)	Zr (g/t)	Pb (g/t)	Cs (g/t)	Th (g/t)	U (g/t)	As (g/t)	Mo (g/t)	Sn (g/t)	Ag (g/t)
	609	176	341	433	90	1.71	6.15	1.71	<20	176.15	47.33	20.2
	Cd (g/t)	W (g/t)	La (g/t)	Ce (g/t)	Pr (g/t)	Nd (g/t)	Sm (g/t)	Eu (g/t)	Gd (g/t)	Tb (g/t)	Dy (g/t)	Ho (g/t)
	3.22	30.8	17.967	40.15	5.14	21.407	4.44	1.293	3.757	0.457	2.6767	0.537
	Er (g/t)	Tm (g/t)	Yb (g/t)	Lu (g/t)	Au (g/t)	Hg (g/t)	Cr (g/t)	S Total (%)	SiO_2 (%)	Al_2O_3 (%)	TiO_2 (%)	Fe_2O_3 (%)
	1.487	0.237	1.533	0.25	<0.02	1.443	35	0.577	62	20.68	0.553	3.26
	CaO (%)	MgO (%)	MnO (%)	Na_2O (%)	K_2O (%)	P_2O_5 (%)	PPC (%)	SO_3 (%)				
	0.527	2.25	0.043	1.057	3.61	0.173	5.177	-				

Note in Table 6A that the composition data show a huge variability: the Cu concentration varies between ~0.05 wt% (Las Tórtolas, Central Chile) and ~1.1 wt% (Northern Chile, Atacama Desert), while other elements such as Fe, Si, Al, Mn, Na, S, Zn, Ni and Au are also present in these flotation tailings. Thus, the copper concentration in flotation tailings is relatively high, especially in northern Chile. This becomes more evident when the concentration data from Table 6A are compared with those shown in Table 3 for copper ores; note in Table 6A that the copper concentration in some flotation tailings (mainly from northern Chile) is similar to the copper concentration in sulfide ores from some Chilean regions (~1wt%—Table 3). According to Table 6B, several critical and valuable metals are present in Chilean flotation tailings, especially V and Sc in Esperanza mine, Nb in Mantos Blancos, W and Sb in Talabre, Y, Ce, La and Nd in Sierra Gorda, and Co in Laguna Seca. Thus, reprocessing tailings may be a promising alternative for recovering critical and valuable metals, in addition to copper. However, this presents some challenges, such as the high iron content (Table 6A) and the large portion of fine particles in the tailings, increasing considerably the costs involved in both liberation and separation processes [17,48].

5. Anode Casting: Smelting and Converting Processes

After the flotation stage, the copper concentrate proceeds to a pyrometallurgical route which involves a smelting step, where a molten high-Cu sulfide matte is obtained, followed by a converting step, where iron and sulfur present in the matte are oxidized, producing blister copper, while also generating dust and slag [95]. The blister copper is forwarded to an anode furnace to be converted into an anode plate (~98.5%–99.6% purity). Finally, the anode proceeds to the electrorefining stage, yielding high-purity copper cathodes (~99.99% purity) by electrolysis in a solution of copper sulfate and sulfuric acid [96].

Seven smelters operate in Chile, one of them owned by Glencore (Altonorte), one owned by Anglo American (Chagres), four owned by Codelco (Chuquicamata, Potrerillos, Ventanas, and Caletones), and one owned by Enami (Hernán Videla Lira). These smelters operate with Flash furnaces, Peirce Smith, Teniente, and Noranda Converters [22,97]. The most important converting technology is the Chilean El Teniente, which has been subjected to several improvements [98–100]. The developments in Chilean processes of copper smelting and converting are presented in the review article published by Devia et al. [22] in 2019.

5.1. Copper Anode

The concentration of impurities in copper anodes has been increasing steadily for several decades due to the increasing extraction of low-grade copper ores. This can be seen in Figure 7, which shows the evolution of the presence of As, Sb, and Bi as impurities in copper anodes over the last 30 years worldwide [101].

Table 7 presents the chemical composition of copper anodes from different Chilean regions. Note that the anodes from all Chilean smelters contain high concentrations of valuable metals, such as Sb, Ni, Au, Ag, Te, and Se; unlike other countries, the concentration of bismuth in Chilean copper anodes is not relevant when compared to the other metals. As all these metals are considered impurities in the copper product, they must be eliminated from the anode in the subsequent steps. Therefore, they will be present in the waste materials generated, from which they can be recovered and used in various applications.

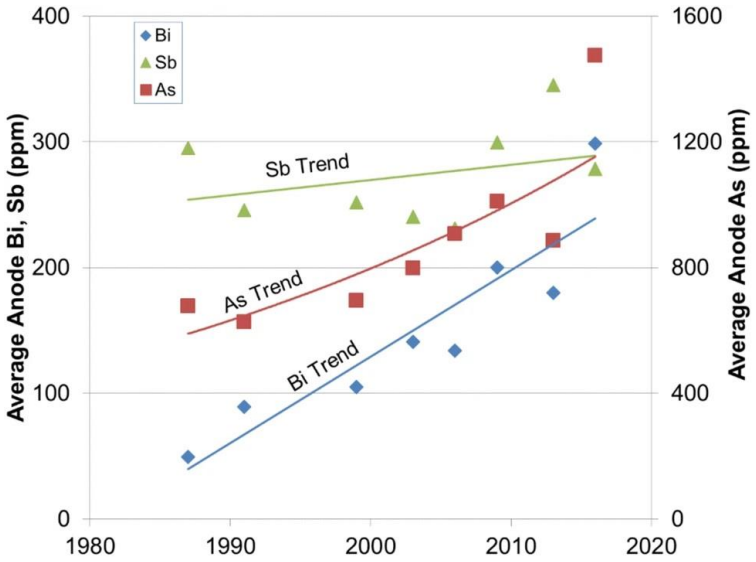

Figure 7. The evolution of the presence of As, Sb, and Bi as impurities in copper anodes over the last 30 years worldwide [101].

Table 7. Chemical composition (in ppm) of copper anodes from Chilean smelters.

Ref.	**[7]**	**[102]**	**[103]**	**[104]**	**[103]**	**[104]**	**[104]**	**[104]**	**[103]**
Smelter	**Chuquicamata**		**El Teniente**	**El Teniente**	**Fundición Hernán Videla Lira**	**Fundición Hernán Videla Lira**	**Fundición Hernán Videla Lira**	**Ventanas**	**Ventanas**
Cu (%)	98.57–99.76		99.62		99.61				99.6
As	365–1587	1200	917.4	952.4	292.48	196.8	169.7	828.2	808.44
Sb	60–235	200	140.95	153.1	52.61	59.3	48.5	609.9	366.38
Bi	6–55	<10	3.45	3.4	5.38	8.4	5.0	8.2	8.14
Fe	6–31	29	12.65	13.4	75.75	43.9	37.6	70	44.8
Ni	13–107	32	138.4	146.2	355.0	657.0	320.2	371.6	256.72
Pb	18–139	<13	37.9	43.7	652.25	1539.0	580.0	453	321.8
S	10–21	29		16.0			20.0	42	
O	1069–1624			1335.0			1641.0	2113	
Au	1–16	1.83	1.2	1.2	29.61	31.7	35.2	30.9	22.84
Ag	155–431	270	133.5	134.0	407.42	469.0	481	717	477.2
Se	86–277	120	218.08	209.1	160.5	164.0	156.3	227	201.0
Te	10–40	33	10.3	10.0	30.33	27.1	27.6	104	53.1
Sn				1.5		5.5	3.1	5.2	

5.2. Smelter and Converter Slag

On the account of transport and disposal costs and in order to maximize the copper production efficiency, managing the slags generated in smelters/converters is one of the major concerns in the copper industry. Generated in the smelting and converting stages, the slag contains, in general, a great amount of copper, which must be recovered [95]. In the El Teniente Converter, for example, the slag is forwarded to the El Teniente Slag Cleaning Furnace Process, which is a batch decoppering process that reduces magnetite and copper contents in the slag. This is achieved through the injection of a solid, liquid or gaseous reductant directly into the equipment. At the Caletones Smelter (Chile), pulverized coal is used as a reductant in the three existing Slag Cleaning Furnaces [91]. Considering the above, several authors have been evaluating methods to reduce slag production and its recycling [26,83,105–107]. Data on the composition of Chilean slags from smelting and converting processes are shown in Table 8. A complete characterization of slags from Paipote Smelter (Chile) may be found in Ref. [108].

Table 8. Chemical composition (%) of slags from Chilean smelters/converters.

Ref.	[109]	[83]	[107]	[110]	[27]	[83]	[91]	[108]	[7]	[83]
Type	**Flash Smelting Furnace**				**Teniente Converter**					**Peirce–Smith Converter**
Smelter/ Converter	**Chuquicamata**	**Unknown**	**Unknown**	**Hernán Videla Lira**	**Chuquicamata**	**Unknown**	**Unknown**	**Hernan Videla Lira**	**Potrerillos**	**Unknown**
Cu	1.61	3.23	2.27	0.75	8.0	7.4	7.2	7.03	8.0	13.3
Fe (total)	35.8		41.3	41.45	38.4	39.4	38.11		38	41.1
Fe_3O_4	7.35	11.8		5.14		18.1	19.73			28.4
Fe_2O_3								15.76		
FeO							27.25	37.79		
SiO_2		27.7		27.89		26.1	37.5	24.19	25	18.9
Si			15.4							
Al			1.6							
Al_2O_3				2.91				3.56		
Ca			0.49							
CaO				2.10				1.26		
MgO				0.88				0.76		
S		3.57	0.83		1.9	2.37	2.38	1.98		0.79
Zn					7.9					
ZnO								2.54		
Pb				0.11	0.1					
Bi					0.1					
As			0.0074		0.4					
Sb					0.06					
Cr_2O_3				0.05						
Cl				0.12						

Note in Table 8 that the slags are mostly composed of iron (~40 wt%), silica (~15–37 wt%), and copper (~0.8–13 wt%). The mass fraction of the latter in the slags is considerably greater than in the copper sulfide ores (Table 3). This, associated with the high concentration of iron, indicates that slags from Chilean smelters/converters are potential resources of raw materials for the copper, iron, and steel industry [6,107]. The most evaluated methods to separate and recover these metals have been atmospheric leaching using different oxidant and leaching agents (acids, alkalis, and salts) [105,111,112], and high pressure oxidative acid leaching [113–115]. However, researchers have shown that these methods present technical limitations, because the high concentration of iron and silica hinders the copper separation [105,116,117]. Therefore, new processes of copper extraction from slags must be developed in the coming years.

5.3. Smelter and Converter Flue Dust

Smelting and converting processes generate flue dust with a high content of copper and impurities, such as As, Sb, Bi, and Zn. Around 60% of the total input of As and 50%–60% of Bi from the flotation concentrate is transferred to the dust [118], which are composed of fine and fragmented particles, and condensed compounds [119]. If dust is directly returned to the smelting furnace, the content of these impurities increases considerably, which reduces the furnace efficiency and hinders the electrorefining process.

The formation of flue dust may be harmful for the population living near smelters due to the contamination of soil, air, and water. Berasaluce et al. [120] evaluated the human health risks involved in the exposure to trace elements in soil and indoor dust in Puchuncaví Valley, Chile. The authors noted high carcinogenic risks due to arsenic exposure, mainly for young children (1–5 years old) in all evaluated regions, and for children (6–18 years old) in the exposed areas. Considering the above-mentioned concerns, several reports on hydrometallurgical routes to treat flue dust from copper smelters/converters have been conducted, and one of the most commonly used techniques for this purpose is leaching with sulfuric acid [23,25,118,121,122]. Table 9 presents the chemical composition of flue dust from some Chilean smelters.

Table 9. Chemical composition (%) of flue dust from Chilean smelters/converters.

Ref.	**[27,28]**	**[123]**	**[124]**	**[119]**
Smelter/Region	**Chuquicamata**	**Unknown**	**Northern Chile**	**Chagres**
Cu	10.4	24.5	5.6	22.98–25.51
Fe	0.8	14	0.3	17.64–22.74
S	10.4		7.2	8.26–11.53
Zn	15.6	0.15	21.3	0.197–0.291
Pb	7.8	0.08	5.7	0.067–0.133
Bi	3.5			0.013–0.043
As	19.4	0.9	10.5	0.82–2.04
Sb	0.1			0.012–0.057
Mo		0.45		0.092–0.190
Al		1.2	0.2	1.3–1.43
Ca			0.3	0.46–0.49
K			1.8	
Mg			0.06	
Na			0.3	
P			<0.1	
Si			1.1	2.92–3.01
Ni				0.004–0.005

The composition data of Chilean flue dust (Table 9) show strong variability in function of the smelter/region; in Chuquicamata, it is mainly composed of As (~20 wt%), Zn (~15 wt%), Cu (~10 wt%), S (~10 wt%), Pb (~8 wt%), and Bi (3.5 wt%). The hydrometallurgical treatment of flue dust has been extensively studied by many authors [23,25,118,121,122],

which is usually conducted to recover copper and to stabilize the impurities; however, the high concentration of arsenic limits this process. Pyrometallurgical routes can also be used to treat As-rich flue dust, for example by roasting it at 750 °C in an oxygen-rich atmosphere. In this case, the commercial-grade As_2O_3 is recovered after cooling the vapors. As_2O_3 is a valuable component in several fields, such as in the production of herbicides, pesticides and in the semiconductor industry. However, its commercialization has faced restrictions in developed countries due to environmental risks [23,118]. Thus, As_2O_3 must be disposed at landfill sites, generating technical and environmental inconveniences. Moreover, pyrometallurgical stages increase the energy consumption and can make the process unfeasible. Thus, new hydrometallurgical processes must be proposed in the coming years to recover copper from flue dusts, especially high-arsenic ones, which are generated in Chuquicamata mine (Table 9).

With composition data of the anode, slag, and flue dust from Chuquicamata mine shown in Tables 7–9, respectively, Figure 8 was constructed. Figure 8 shows the distribution (mass fraction) of Cu, Fe, As, Sb, and Bi, in the three materials generated in the smelting and converting stages. Note that the fraction of copper in the slag and dust is similar, indicating that both are potential sources of copper. The valuable Sb and mainly Bi metals are mostly present in the dust, which means that effective methods to recover both metals from this material need to be evaluated. In this case, the large amount of As must be considered since it may hinder the separation of the metals. The slag also shows to be a valuable resource of Sb and, in this case, the high concentration of Fe needs to be considered.

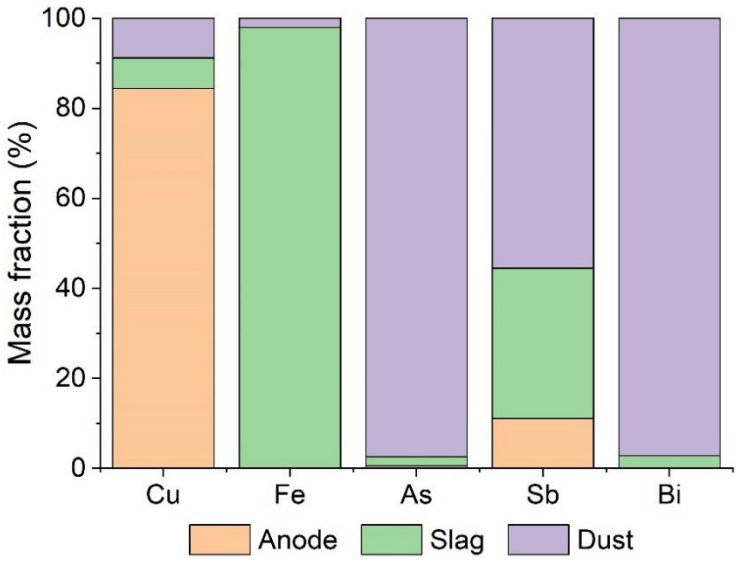

Figure 8. Distribution (mass fraction) of Cu, Fe, As, Sb and Bi present in the anode, slag, and flue dust from Chuquicamata mine.

6. Copper Electrorefining

Since the pyrometallurgical route is unable to remove the impurities from the copper concentrate completely, copper anodes from the smelting/converting stages must be submitted to the electrorefining process. In this stage, the anode is immersed in a tank containing an acid electrolyte and a cathode so that the copper from the anode is deposited onto the cathode. However, some impurities that could not be eliminated in previous stages are also released from the anode. Some of the impurities dissolve in the electrolyte, while others form a slime at the bottom of the cell, which is referred to as anode slime. Lastly, part of the copper is not oxidized in the electrorefining process and remains at the anode, being called anode scrap.

6.1. Anode Scrap

In the electrorefining stage, approximately 85% by weight of the copper present at the anode is oxidized, while 15% is not dissolved and remains at the anode, which is referred to as anode scrap [125]. The anode scrap is generated mainly due to the inhomogeneous morphology of the anode and its passivation [126]. Furthermore, there is also a significant part of the anode that connects to the power source, which makes it unable to be completely submerged into the electrolyte, and in turn has to return to the process as anode scrap [125]. The greater the amount of anode scrap, the greater the energy consumption, which is minimized by casting thick and equal mass anodes, and by equalizing the current between all anodes and cathodes [7].

Anode scraps are typically washed, dried, remelted, and cast into new anodes that are then resent to the electrorefining stage [7,127]. In recent years, some authors have evaluated methods that reduce the formation of anode scraps or alternative techniques that enable copper recovery. Loira and Mikenberg [128] evaluated the substitution of the conventional copper anodes by bar-shaped anodes coming from an extrusion and wire drawing process, which improved the surface quality and homogeneity of the copper anode. Cifuentes et al. [125,129] have conducted modeling and experimental studies to evaluate the use of electro-electrodialysis in the recovery of copper from anode scraps; in this case, copper ions are oxidized from the anode, migrate across a cation-exchange membrane, and deposit at the cathode. The cation-exchange membrane was present in the system to prevent the cathode contamination by the sludge formed during the metal oxidation. Although copper was recovered from the anode scrap, the energy consumption was between three and four times greater than that of the conventional process without an ion-exchange membrane; therefore, conducting additional studies is needed.

Although information on chemical composition of anode scraps is scarce in the literature—from the best of our knowledge, there is no composition data of Chilean anode scraps reported—data on chemical composition of anode scraps from a refinery from the USA may be found in Ref. [130].

6.2. Anode Slime

While copper from the anode dissolves in the electrolyte and deposits at the cathode, impurities do not dissolve and sediment at the bottom of the electrolysis cell; this material is referred to as anode slime [30]. The quantity, morphology, pore structure, and adhesion properties of the slimes are factors that must be evaluated because they affect the mass transfer mechanisms at the anode/electrolyte interface considerably [131]. The concentration of As, Sb, and Bi in the anode slime is particularly important. As will be presented in Section 6.3, high levels of As are usually maintained in the electrolyte to allow the precipitation of Sb and Bi into the slime, preventing cathode contamination [7,31,132]. On the other hand, its toxicity raises concerns regarding human health.

After an electrorefining cycle, the slime is drained from the bottom of the cell and forwarded to the recovery of copper and byproducts. Several authors have evaluated methods to reduce anode slime formation or alternative techniques to recover copper and valuable metals from it, as shown in the review articles recently published [127,133–135]. Table 10 presents the composition of anode slimes from Chilean companies. The significant variation of composition data shown in the table may be explained by the strong dependence of anode slimes composition on the mineral raw materials, composition of copper anode (Table 7), casting quality, and technical conditions of electrolysis. Despite these variations, note in Table 10 that the anode slimes from most Chilean refineries contain high mass fraction of copper and other valuable metals, such as Sb, Se, Ag, Au, with Ni, Bi and Te in lower concentrations. This has encouraged authors to conduct extensive research on the recovery of valuable metals from anode slimes, involving basically four broad categories of processes: pyrometallurgy, partial hydrometallurgy, surface chemical (e.g., flotation) and physical separation processes, and hydrometallurgical processes [133]. These processes present several limitations, as shown in Refs. [127,133–135]. According to Liu et al. [133],

the major difficulties in the treatment of anode slimes are low precious metal recovery rate, high consumption of chemicals, and large amounts of residues generated. Hydrometallurgical processes show additional challenges, such as the lack of solvents able to leach all the elements present in the slime, the toxicity of reagents, the need to treat the wastes before their final disposal in the environment, and the long times required. To overcome these limitations, metallurgical methods should be developed in the coming years involving, for example, metal–organic frameworks (MOFs), supercritical technology, vacuum metallurgy technology, biological metallurgy, ion exchange technologies, electrochemical processes, and the use of new materials such as graphene and nanoparticles [133,135]. Liu et al. [133] also emphasized the importance of the role of governments in strengthening policies of precious metals recovering from anode slimes since they are rich metal resources, as shown in Table 10, and have great economic value. Thus, the governments should implement a loose tax policy to encourage industries to explore copper anode slimes.

Table 10. Composition (wt%) of Chilean anode slimes.

Ref.	[134]	[102]	[134]	[104]	[104]	[104]	[136]	[136]
Refinery	**Chuquicamata**	**Chuquicamata**	**El Salvador**	**Fundición Hernán Videla Lira**	**El Teniente**	**Ventanas**	**Ventanas**	**Potrerillos**
Cu	27	22.9	5	19.8	28.8	12.05	24.27	7.8
As	5	6.6	0.7	1.51	9.2	2	6.2	9.22
Sb	4	5.56	3	0.058	8.06	0.18	5.5	10.45
Bi		0.21		0.19	0.29	0.12	0.3	0.41
Te		0.59		0.77	0.14	0.82	0.8	0.66
Fe		0.29		0.26	0.07	0.21	0.1	0.19
Pb		0.52		32.2	1.76	23.25	8.1	1.16
Ni		0.02		0.43	0.12	0.68	0.1	0.02
Se	4	4.92	21	3.9	9.3	3.14	7.9	8.65
Ag	12	21.9	24				14.77	15.42
Au	0.07	0.14	1.4	7.74	0.47	11.34	5.4	0.47
Zn				0.077	0.02	0.1		
Mg					0.004	0.01		
Ca				0.3	4.14	0.6		
Al		0.44						
SO_4		7.8						
SiO_2		6.94						
P		<0.02						
Cl		1.06			0.7			

6.3. Acid Electrolyte

The tankhouse electrolyte is composed of sulfuric acid, copper sulfate, and some additives that control the structure and morphology of the deposits, such as thiourea, glue, and chloride ions [7,137]. Copper ions migrate from the anode towards the cathode, which is the product of the overall process (99.99% purity). However, some impurities present at the anode, such as As, Sb, Bi, S, Fe, Zn, Ni, and Co, can affect negatively the electrorefining stage as these elements dissolve into the electrolyte [96]. Among them, Sb and Bi cause major concerns since they have standard reduction potentials similar to that of copper [138]. This may reduce the cathode purity, cause the passivation of the anode, and intensify the anode slime formation [30,40,139]. Therefore, part of the electrolyte is continuously bled from the tankhouse and forwarded to a set of electrowinning cells in order to be treated [132]. This method presents some drawbacks, such as high energy consumption and the formation of toxic arsine gas [31]. Another technique conventionally used in this industry comprises the addition of As in the electrolyte, which leads to the deposition of Sb and Bi into the anode slime (Table 10) due to the reduction in their solubility [34,35].

However, this method presents health concerns due to the toxicity of arsenic. Furthermore, the valuable antimony and bismuth metals are lost in the formed slime [132].

Antimony and bismuth have been considered as critical metals [32,140], which has been intensified by China's dominance in their production; it accounts for about 90% and 75% of the world's production of Sb and Bi, respectively [32,141], causing concerns due to the several applications of these valuable metals. Antimony is an important constituent of lead-acid batteries, and its major use is for flame-retardants. It is also used as a catalyst for PET production, in the electronic industry, in pesticides, medicines, detonators, glass decolorizers, ammunitions, and pigments. Lead-antimony alloys have also several applications, such as in corrosion-resistant pumps and pipes, roofing sheets, solder, and cables [33,141,142]. In addition to some above-mentioned applications, bismuth is used in cosmetics and in the pharmaceutical industry [143,144]. Bi-Sb alloys are also used as semiconductors in electronics [145]. The widespread use of antimony and bismuth and the growing concerns regarding their scarcity point to the need to recover these metals in the copper electrorefining stage. In Chile, the impurities responsible for the greatest incidence of cathode contamination and operational problems are As and Sb [96]; the concentration of Bi in Chilean electrolytes is usually very low [36,38].

Considering the limitations of the conventional techniques used to treat tankhouse electrolytes, several authors have evaluated alternative methods, such as solvent displacement crystallisation [146,147], solvent extraction [36,37], activated carbon [38,39], chemical leaching [40], electrodialysis [41], electrowinning [32], and ion-exchange resins [30,42]. Among these techniques, ion-exchange resins have shown special relevance in the literature, in addition to already being used in industries worldwide [30]. Henceforth, we will focus on the use of ion-exchange resins to treat copper electrolytes.

Table 11 presents the concentration of Chilean electrolytes from the electrorefining stage, which are composed mainly of H_2SO_4 (~200 g/L), Cu (~45 g/L), and some impurities, such as As (~6–21 g/L), Ni (~18 g/L), Sb (~0.2–0.6 g/L), and Fe (~0.2 g/L). It is worth mentioning that the concentration of bismuth shown in Ref. [148] differs considerably from the Chilean data presented in the other works.

Table 11. Concentration (in g/L) of Chilean electrolytes from the electrorefining stage of copper production.

Ref.	[38]	[96,149]	[148]
H_2SO_4 (g/L)	160	220	202.2
Cu (g/L)	45.6	39.4	45.5
As (g/L)	21.2	9.76	6.4
Sb (g/L)	0.44	0.2167	0.58
Bi (g/L)			0.60
Ni (g/L)			18.2
Fe (g/L)		0.174	

7. Ion-Exchange Resins

Amino-phosphonic resins have been extensively tested on laboratory and industrial scale worldwide to remove mainly antimony and bismuth from contaminated copper electrolytes [30,42,150–153]. In general, the most evaluated factors in these studies are the mass of resins, the contact time, and the concentration of metals. In addition to these parameters, researchers have been evaluating the influence of the temperature [154], the use of thiourea as an additive [30], the oxidation from Sb(III) to Sb(V) [42], the precipitation of species in the resin pores [150], the poisoning of the resins by ferric ions, and washing procedures of the resin before the elution stage [30].

7.1. Clean Electrolyte after Passing through Ion-Exchange Resins

To the best of our knowledge, few data on the chemical composition of real solutions leaving ion-exchange resins from Chilean factories are reported in the literature.

Cifuentes et al. [149] evaluated the removal of antimony from Chilean copper electrolytes on a laboratory scale using three ion-exchange resins: MX-2 (Jacobi Resinex, Osaka, Japan), UR-3300S (Unitika, Osaka, Japan), and Duolite C-467 (DuPont, Wilmington, IL, USA). The contaminated electrolyte tested by the authors came from a refinery located in the north of Chile and presented the composition shown in Table 12. Concentration data for the clean solution that left the resin over time are shown in Table 13. Even though only the data regarding Sb ions were reported, it is worth mentioning that all copper ions that entered the resin were expected to leave it, whereas a part of the ferric ions has probably been adsorbed by the resin. On another report, Cifuentes et al. [96] evaluated the same three ion-exchange resins for treating a Chilean contaminated electrolyte: the authors obtained very similar results on the concentration of Sb that left the resin to those shown in Table 13. Note in the table that the resin UR-3300S behaves very differently from the MX-2 and Duolite C-467, which indicates that the UR-3300S presents greater antimony extraction capacity than the other resins. Composition data on clean electrolytes from Japan [155] and Spain [30] leaving ion-exchange resins can also be found in the literature.

Table 12. Initial concentration (in g/L) of the Chilean contaminated electrolyte treated by Cifuentes et al. [96] using ion-exchange resins.

H_2SO_4	Cu	Sb	Fe	As
220	39.4	0.2167	0.174	9.76

Table 13. Concentration of Sb (in g/L) in Chilean clean solutions that left the ion-exchange resins tested by Cifuentes et al. [96].

	Sb Concentration (g/L)		
Time (h)	MX-2	UR-3300S	Duolite C-467
1	0.0296	0.0366	0.0398
2	0.1025	0.0544	0.1085
3	0.1071	0.0615	0.117
4	0.1095	0.0616	0.1139
5	0.1195	0.0605	0.1175
6	0.1198	0.0611	0.1186
7	0.1201	0.0617	0.1191
8	0.1201	0.0619	0.1189

7.2. Elution Solution from Ion-Exchange Membranes

After passing the electrolyte through the ion-exchange resin, the adsorbed species must be extracted from the resin. Therefore, an elution process is conducted, in which the resin is regenerated by ion exchange between protons and the impurities adsorbed, such as Sb and Bi. In general, the elution is performed with HCl solutions at concentrations of 5–7 mol/L [101,154], where the metals are eluted as complex chlorine-based anions ($SbCl_4^-$ and $BiCl_4^-$). In Chilean refineries, the main species eluted is antimony, because the concentration of bismuth is extremely low, as mentioned previously.

In recent years, several authors have studied the factors that affect the elution stage in order to enhance the desorption of metals and the lifetime of the resins. One of the evaluations often conducted is the poisoning phenomenon and the inactivation of the resin after several cycles of adsorption and elution. According to Riveros et al. [150], this occurs mainly due to the much lower elution rate of Sb(V) compared to Sb(III). Therefore, Sb(V) ions tend to accumulate in the resin, decreasing its loading capacity and hindering the next adsorption cycles. To overcome this limitation, the use of thiourea in the HCl solution has been tested and very promising results have been obtained. In the study conducted by Riveros et al. [156], the use of thiourea in a concentration of at least 0.002 mol/L increased considerably the elution rate of Sb(V). Similar results were obtained by Kryst

and Simmons [157], who suggested that this improvement of the Sb elution rate using thiourea occurred due to the reduction of Sb(V) to Sb(III). This suggestion on the reduction of Sb(V) by thiourea was supported in the study performed by Riveros et al. [42]. Recently, Arroyo-Torralvo et al. [30] tested the use of several additives in the elution stage together with HCl, such as thiourea, CuCl, NaCl, and thiourea with CuCl. Among them, the use of thiourea in 1 g/L showed to be the most promising additive to eluate Sb and Bi from the resin. Another advantage of using thiourea in the elution process is that this component is usually available in refineries since it is used to improve the quality of the cathodes. However, researchers still need to study the Sb desorption mechanisms in depth in addition to conducting tests on an industrial scale.

As mentioned in Section 7.1, chemical composition data of solutions from ion-exchange resin processes in the electrorefining stage are scarce in the literature. Since no data for elution solutions from industrial processes were found during this research, composition data of antimony in elution solutions obtained in tests conducted by authors worldwide are shown in Table 14. Some of these data were extracted from figures, and others from tables. The origin of the contaminated electrolytes tested in Refs. [42,150,156] is unknown, whereas the study presented in Ref. [30] was performed with solutions from a Spanish refinery. In Ref. [30] composition data of bismuth were also reported. Solutions of HCl ranging from 4 to 6.7 mol/L were used as eluent agent in the investigations compiled in Table 14.

Table 14. Concentration of Sb and Bi (in g/L) in HCl elution solutions leaving ion-exchange resins.

[156]		[42]		[150]		[30]		
Time (h)	**Sb (g/L)**	**Bed Volume**	**Sb (g/L)**	**Bed Volume**	**Sb (g/L)**	**Cycle**	**Sb (g/L)**	**Bi (g/L)**
6	0.021	0	0.000	0	0.000	1	1.233	1.000
12	0.056	1.1	0.148	0.6	0.013	2	1.367	0.933
18	0.049	3.0	0.579	1.7	0.013	4	1.133	0.667
24	0.043	4.7	0.613	2.8	0.168	5	1.083	0.667
29	0.040	6.5	0.279	3.9	0.946	6	1.217	0.633
46	0.032	8.2	0.099	5.1	2.290	7	1.067	0.517
57	0.026	10	0.030	6.2	1.740	8	1.133	0.517
71	0.021	11.7	0.010	7.3	1.080	9	0.933	0.467
78	0.019	13.7	0.003	8.5	0.712	10	1.000	0.417
94	0.016	15.8	0.000	9.7	0.505			
		18.9	0.000	10.8	0.376			
		21.8	0.000	12.1	0.207			
				15.0	0.052			
				17.1	0.000			

As shown in Table 14, the elution solution from ion-exchange resins is a valuable resource of antimony and bismuth, and this has not yet been widely explored in the literature. In general, after the elution step, the HCl solution containing the metals (mainly Sb for Chilean electrolytes) is forwarded to the HCl recovery stage, which is conventionally carried out by fractional distillation. This method generates gaseous Cl_2, which is corrosive and harmful to human health. Therefore, the recovery of HCl from the elution process using reactive electrodialysis has been evaluated [138]; however, antimony and bismuth were not added to the HCl solutions evaluated in that study. This indicates that studies on the recovery of Sb and Bi present in the elution solution are needed, and the use of the reactive electrodialysis technique for this purpose may be promising since it allows the HCl recycling, which can return to the elution step, simultaneously to the recovery of the valuable Sb and Bi metals. Thus, additional studies must be conducted considering the presence of Sb and Bi in the HCl solutions, besides evaluating the influence of operational parameters, such as metals concentration, pH, electrode material, membrane type, and applied current density. Other methods able to separate Sb and Bi from the HCl solution are also expected to be tested in the coming years.

8. Conclusions and Perspectives

According to the literature, in the coming years, Chilean mining companies will face significant challenges, such as ore grade decline, increase in energy and water consumption, and the need to expand and construct new tailings dams. Furthermore, the risk of a supply crisis of critical metals, such as antimony and bismuth, will encourage companies to extract these metals from secondary resources in copper production. In order to conduct studies on the development of new technologies able to overcome these challenges, it is crucial to know the chemical composition data of each stage of the process. Thus, the present paper provides a review of composition data of the main stages of Chilean copper production from sulfide minerals and the recent advances in the development of technologies for copper mining reported in the literature.

A summary of the copper concentration ranges in the main Chilean copper production steps is shown in Figure 9. Concentration data of antimony are also shown in the figure, since the recovery of this valuable metal as a secondary resource in copper production has been evaluated intensively in recent years. In addition to Sb, several other valuable metals such as Se, Te, Au, Ag and Ni are present in significant amounts in the waste materials generated, such as flotation tailings, slags and flue dust from the smelting/converting stage, anode slime and contaminated electrolyte from the electrorefining stage, in addition to the elution solution from the ion-exchange resins. The results shown in the present paper point to urgent need to conduct more studies aimed at developing new technologies capable of increasing the efficiency of copper production. This will make the copper production more competitive, will favor the recovery of critical metals that are at risk of becoming depleted in the coming years, will reduce the environmental concerns associated with areas occupied by tailings, will reduce the risks of contamination with dangerous metals, and will favor the circular economy. Optimizing copper production in the coming years is especially important for the Chilean economy since this country is strongly dependent on copper production and several authors have estimated that it will decrease from 2030 due to the lack of technologies that would make the copper production technically, economically, and environmentally viable.

There is a large number of potential directions for future works on optimization of copper production. One of them is the reduction of energy consumption of the comminution process, because this stage is one of the major responsible for the operational costs of mining industry, which tend to increase in the coming years due to the ore grade decline. To conduct these studies, authors need to develop techniques to quantify trace elements in copper ores, because these data are scarce in the literature and the mineralogical composition strongly influences the comminution performance. It is also expected that new investigations on flotation will be developed to increase the process efficiency and minimize the generation of tailings. In addition, studies on the extraction of valuable metals present in flotation tailings, such as Sb, V, Sc, Nb, W, Y, Ce, La and Nd, should be carried out. For this, authors need to consider the high concentration of iron and the large portion of fine particles in the tailings, which hinder the extraction of metals. Investigations on copper recovery from slags generated in smelters/converters are also expected to intensify in the coming years. In this case, authors must develop alternative techniques since the conventional atmospheric leaching is limited by the high concentration of iron and silica in the slag. Studies involving copper recovery from flue dusts should also be intensified but, in this case, the high concentration of As must be considered. Investigations on the extraction of valuable metals from slags and flue dusts, such as Sb and Bi, respectively, should also be conducted. Lastly, several studies regarding the electrorefining stage are expected to be carried out in the coming years, involving mainly (i) alternative methods to treat anode slimes considering the low precious metal recovery rate, high consumption of chemicals, and large amounts of residues generated; (ii) techniques to treat tankhouse electrolytes, especially ion-exchange resins; and (iii) methods such as electromembrane processes to recover Sb and Bi present in the elution solution from the ion-exchange resins.

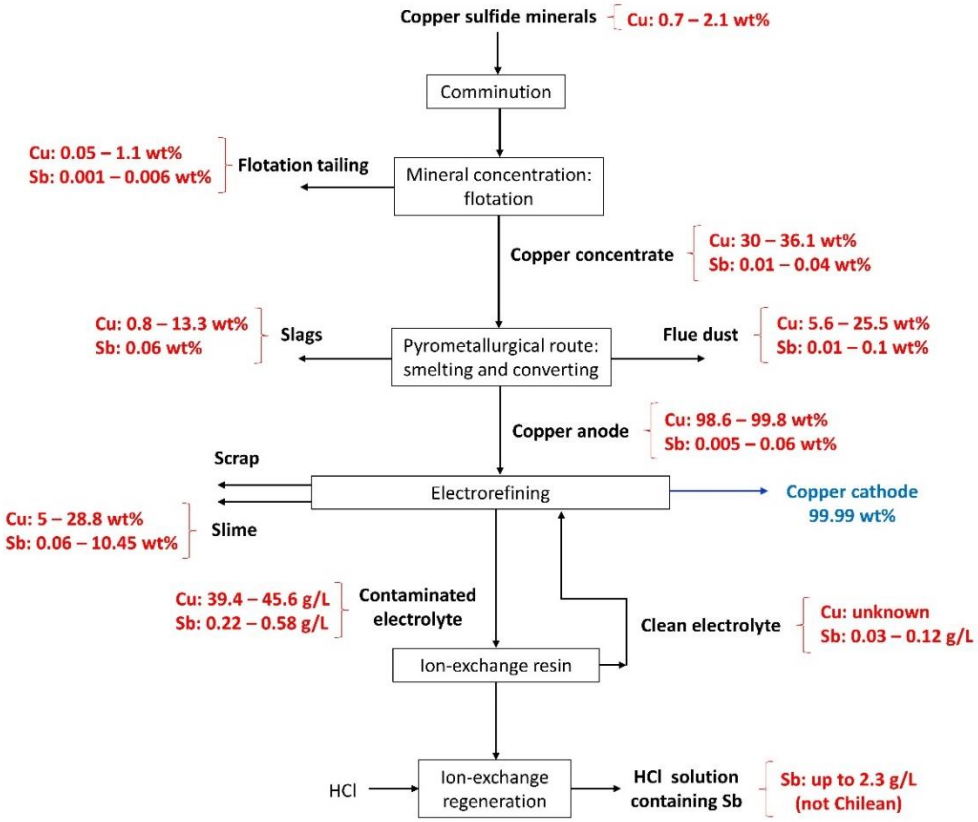

Figure 9. Flowchart of the copper production from sulfide minerals showing the concentration ranges of copper and antimony in the main Chilean process stages.

Author Contributions: Conceptualization, K.S.B. and A.M.B.; methodology, K.S.B. and A.M.B.; investigation, K.S.B.; data curation, K.S.B.; writing—original draft preparation, K.S.B.; writing—review and editing, K.S.B., V.S.V., B.G.M., G.C. and A.M.B.; visualization, K.S.B. and A.M.B.; supervision, A.M.B.; project administration, A.M.B.; funding acquisition, G.C., G.R. and A.M.B. All authors have read and agreed to the published version of the manuscript.

Funding: This research was funded by CNPq (Process 160320/2019-4), Cyted (Network 318RT0551), ERAMIN2 (Network Sb-RECMEMTEC, FINEP—Brazil, ANID—Chile, and AEI—Spain) and Dirección de Investigación Científica y Tecnológica (DICYT) of the Universidad de Santiago de Chile. This study was financed in part by the Coordenação de Aperfeiçoamento de Pessoal de Nível Superior—Brasil (CAPES)—Finance Code 001 (Process 88887.364537/2019-00).

Conflicts of Interest: The funders had no role in the design of the study; in the collection, analyses, or interpretation of data; in the writing of the manuscript, or in the decision to publish the results.

References

1. Dini, J.W.; Snyder, D.D. Electrodeposition of Copper. In *Modern Electroplating*; John Wiley & Sons, Inc.: Hoboken, NJ, USA, 2011; pp. 33–78.
2. Yin, Z.; Sun, W.; Hu, Y.; Zhang, C.; Guan, Q.; Wu, K. Evaluation of the possibility of copper recovery from tailings by flotation through bench-scale, commissioning, and industrial tests. *J. Clean. Prod.* **2018**, *171*, 1039–1048. [CrossRef]
3. Endres, F.; Abbott, A.; MacFarlane, D.R. *Electrodeposition from Ionic Liquids*; Wiley-VCH: Weinheim, Germany, 2008; Volume 1, ISBN 978-3-527-31565-9.
4. Saidi, M.; Kadkhodayan, H. Experimental and simulation study of copper recovery process from copper oxide ore using aspen plus software: Optimization and sensitivity analysis of effective parameters. *J. Environ. Chem. Eng.* **2020**, *8*, 103772. [CrossRef]
5. Lagos, G.; Peters, D.; Lima, M.; Jara, J.J. Potential copper production through 2035 in Chile. *Miner. Econ.* **2020**, *33*, 43–56. [CrossRef]
6. Palacios, J.; Sánchez, M. Wastes as resources: Update on recovery of valuable metals from copper slags. *Trans. Institutions Min. Metall. Sect. C Miner. Process. Extr. Metall.* **2011**, *120*, 218–223. [CrossRef]

7. Schlesinger, M.E.; King, M.J.; Sole, K.C.; Davenport, W.G. *Extractive Metallurgy of Copper*; Elsevier: Amsterdam, The Netherlands, 2011; Volume 53, ISBN 9780080967899.
8. Reyes-Bozo, L.; Godoy-Faúndez, A.; Herrera-Urbina, R.; Higueras, P.; Salazar, J.L.; Valdés-González, H.; Vyhmeister, E.; Antizar-Ladislao, B. Greening chilean copper mining operations through industrial ecology strategies. *J. Clean. Prod.* **2014**, *84*, 671–679. [CrossRef]
9. Xu, W.; Dhawan, N.; Lin, C.L.; Miller, J.D. Further study of grain boundary fracture in the breakage of single multiphase particles using X-ray microtomography procedures. *Miner. Eng.* **2013**, *46–47*, 89–94. [CrossRef]
10. Aldrich, C. Consumption of steel grinding media in mills—A review. *Miner. Eng.* **2013**, *49*, 77–91. [CrossRef]
11. Pamparana, G.; Kracht, W.; Haas, J.; Díaz-Ferrán, G.; Palma-Behnke, R.; Román, R. Integrating photovoltaic solar energy and a battery energy storage system to operate a semi-autogenous grinding mill. *J. Clean. Prod.* **2017**, *165*, 273–280. [CrossRef]
12. Curry, J.A.; Ismay, M.J.L.; Jameson, G.J. Mine operating costs and the potential impacts of energy and grinding. *Miner. Eng.* **2014**, *56*, 70–80. [CrossRef]
13. Jacob, W.; Cooper, D.R.; Gutowski, T.; Ramos-Grez, J. The efficiency of copper ore comminution: A thermodynamic exergy analysis. *Miner. Eng.* **2017**, *109*, 21–31. [CrossRef]
14. Agheli, S.; Hassanzadeh, A.; Hassas, B.V.; Hasanzadeh, M. Effect of pyrite content of feed and configuration of locked particles on rougher flotation of copper in low and high pyritic ore types. *Int. J. Min. Sci. Technol.* **2018**, *28*, 167–176. [CrossRef]
15. Vaziri Hassas, B.; Caliskan, H.; Guven, O.; Karakas, F.; Cinar, M.; Celik, M.S. Effect of roughness and shape factor on flotation characteristics of glass beads. *Colloids Surf. A Physicochem. Eng. Asp.* **2016**, *492*, 88–99. [CrossRef]
16. Han, B.; Altansukh, B.; Haga, K.; Stevanović, Z.; Jonović, R.; Avramović, L.; Urosević, D.; Takasaki, Y.; Masuda, N.; Ishiyama, D.; et al. Development of copper recovery process from flotation tailings by a combined method of high-pressure leaching-solvent extraction. *J. Hazard. Mater.* **2018**, *352*, 192–203. [CrossRef] [PubMed]
17. Mackay, I.; Videla, A.R.; Brito-Parada, P.R. The link between particle size and froth stability—Implications for reprocessing of flotation tailings. *J. Clean. Prod.* **2020**, *242*, 118436. [CrossRef]
18. Santander, M.; Valderrama, L. Recovery of pyrite from copper tailings by flotation. *J. Mater. Res. Technol.* **2019**, *8*, 4312–4317. [CrossRef]
19. Escobar, B.; Quiroz, L.; Vargas, T. Effect of Flotation and Solvent Extraction Reagents on the Bioleaching of a Copper Concentrate with *Sulfolobus Metallicus*. *Adv. Mater. Res.* **2009**, *71–73*, 421–424. [CrossRef]
20. Mackay, I.; Mendez, E.; Molina, I.; Videla, A.R.; Cilliers, J.J.; Brito-Parada, P.R. Dynamic froth stability of copper flotation tailings. *Miner. Eng.* **2018**, *124*, 103–107. [CrossRef]
21. Tabosa, E.; Rubio, J. Flotation of copper sulphides assisted by high intensity conditioning (HIC) and concentrate recirculation. *Miner. Eng.* **2010**, *23*, 1198–1206. [CrossRef]
22. Devia, M.; Parra, R.; Queirolo, C.; Sánchez, M.; Wilkomirsky, I. Copper smelting and converting: Past and present Chilean developments. *Miner. Process. Extr. Metall. Trans. Inst. Min. Metall.* **2019**, *128*, 108–116. [CrossRef]
23. Jarošíková, A.; Ettler, V.; Mihaljevič, M.; Drahota, P.; Culka, A.; Racek, M. Characterization and pH-dependent environmental stability of arsenic trioxide-containing copper smelter flue dust. *J. Environ. Manag.* **2018**, *209*, 71–80. [CrossRef]
24. Xu, Z.F.; Li, Q.; Nie, H.P. Pressure leaching technique of smelter dust with high-copper and high-arsenic. *Trans. Nonferrous Met. Soc. China* **2010**, *20*, s176–s181. (In English) [CrossRef]
25. Ha, T.K.; Kwon, B.H.; Park, K.S.; Mohapatra, D. Selective leaching and recovery of bismuth as Bi_2O_3 from copper smelter converter dust. *Sep. Purif. Technol.* **2015**, *142*, 116–122. [CrossRef]
26. González, C.; Parra, R.; Klenovcanova, A.; Imris, I.; Sánchez, M. Reduction of Chilean copper slags: A case of waste management project. *Scand. J. Metall.* **2005**, *34*, 143–149. [CrossRef]
27. Montenegro, V.; Sano, H.; Fujisawa, T. Recirculation of chilean copper smelting dust with high arsenic content to the smelting process. *Mater. Trans.* **2008**, *49*, 2112–2118. [CrossRef]
28. Montenegro, V.; Sano, H.; Fujisawa, T. Recirculation of high arsenic content copper smelting dust to smelting and converting processes. *Miner. Eng.* **2013**, *49*, 184–189. [CrossRef]
29. Wilkomirsky, I.; Parra, R.; Parada, F.; Balladares, E. Continuous Converting of Copper Matte to Blister Copper in a High-Intensity Molten-Layer Reactor. *JOM* **2014**, *66*, 1687–1693. [CrossRef]
30. Arroyo-Torralvo, F.; Rodríguez-Almansa, A.; Ruiz, I.; González, I.; Ríos, G.; Fernández-Pereira, C.; Vilches-Arenas, L.F. Optimizing operating conditions in an ion-exchange column treatment applied to the removal of Sb and Bi impurities from an electrolyte of a copper electro-refining plant. *Hydrometallurgy* **2017**, *171*, 285–297. [CrossRef]
31. Wang, X.; Chen, Q.; Yin, Z.; Wang, M.; Xiao, B.; Zhang, F. Homogeneous precipitation of As, Sb and Bi impurities in copper electrolyte during electrorefining. *Hydrometallurgy* **2011**, *105*, 355–358. [CrossRef]
32. Thanu, V.R.C.; Jayakumar, M. Electrochemical recovery of antimony and bismuth from spent electrolytes. *Sep. Purif. Technol.* **2020**, *235*, 116169. [CrossRef]
33. Yellishetty, M.; Huston, D.; Graedel, T.E.; Werner, T.T.; Reck, B.K.; Mudd, G.M. Quantifying the potential for recoverable resources of gallium, germanium and antimony as companion metals in Australia. *Ore Geol. Rev.* **2017**, *82*, 148–159. [CrossRef]
34. Xiao, F.; Mao, J.; Cao, D.; Shen, X.; Volinsky, A.A. The role of trivalent arsenic in removal of antimony and bismuth impurities from copper electrolytes. *Hydrometallurgy* **2012**, *125–126*, 76–80. [CrossRef]

35. Wang, X.W.; Chen, Q.Y.; Yin, Z.L.; Wang, M.Y.; Tang, F. The role of arsenic in the homogeneous precipitation of As, Sb and Bi impurities in copper electrolyte. *Hydrometallurgy* **2011**, *108*, 199–204. [CrossRef]
36. Navarro, P.; Simpson, J.; Alguacil, F.J. Removal of antimony (III) from copper in sulphuric acid solutions by solvent extraction with LIX 1104SM. *Hydrometallurgy* **1999**, *53*, 121–131. [CrossRef]
37. Artzer, A.; Moats, M.; Bender, J. Removal of Antimony and Bismuth from Copper Electrorefining Electrolyte: Part II—An Investigation of Two Proprietary Solvent Extraction Extractants. *JOM* **2018**, *70*, 2856–2863. [CrossRef]
38. Navarro, P.; Alguacil, F.J. Adsorption of antimony and arsenic from a copper electrorefining solution onto activated carbon. *Hydrometallurgy* **2002**, *66*, 101–105. [CrossRef]
39. Salari, K.; Hashemian, S.; Baei, M.T. Sb(V) removal from copper electrorefining electrolyte: Comparative study by different sorbents. *Trans. Nonferrous Met. Soc. China* **2017**, *27*, 440–449. [CrossRef]
40. Awe, S.A.; Sandström, K. Selective leaching of arsenic and antimony from a tetrahedrite rich complex sulphide concentrate using alkaline sulphide solution. *Miner. Eng.* **2010**, *23*, 1227–1236. [CrossRef]
41. Cifuentes, L.; Crisóstomo, G.; Ibáñez, J.P.; Casas, J.M.; Alvarez, F.; Cifuentes, G. On the electrodialysis of aqueous H_2SO_4-$CuSO_4$ electrolytes with metallic impurities. *J. Memb. Sci.* **2002**, *207*, 1–16. [CrossRef]
42. Riveros, P.A. The removal of antimony from copper electrolytes using amino-phosphonic resins: Improving the elution of pentavalent antimony. *Hydrometallurgy* **2010**, *105*, 110–114. [CrossRef]
43. Haas, J.; Moreno-Leiva, S.; Junne, T.; Chen, P.J.; Pamparana, G.; Nowak, W.; Kracht, W.; Ortiz, J.M. Copper mining: 100% solar electricity by 2030? *Appl. Energy* **2020**, *262*, 114506. [CrossRef]
44. Lam, E.J.; Cánovas, M.; Gálvez, M.E.; Montofré, Í.L.; Keith, B.F.; Faz, Á. Evaluation of the phytoremediation potential of native plants growing on a copper mine tailing in northern Chile. *J. Geochem. Explor.* **2017**, *182*, 210–217. [CrossRef]
45. Northey, S.; Mohr, S.; Mudd, G.M.; Weng, Z.; Giurco, D. Modelling future copper ore grade decline based on a detailed assessment of copper resources and mining. *Resour. Conserv. Recycl.* **2014**, *83*, 190–201. [CrossRef]
46. Lagos, G.; Peters, D.; Videla, A.; Jara, J.J. The effect of mine aging on the evolution of environmental footprint indicators in the Chilean copper mining industry 2001–2015. *J. Clean. Prod.* **2018**, *174*, 389–400. [CrossRef]
47. De Solminihac, H.; Gonzales, L.E.; Cerda, R. Copper mining productivity: Lessons from Chile. *J. Policy Model.* **2018**, *40*, 182–193. [CrossRef]
48. Alcalde, J.; Kelm, U.; Vergara, D. Historical assessment of metal recovery potential from old mine tailings: A study case for porphyry copper tailings, Chile. *Miner. Eng.* **2018**, *127*, 334–338. [CrossRef]
49. Fuentes, G.; Viñals, J.; Herreros, O. Hydrothermal purification and enrichment of Chilean copper concentrates. Part 1: The behavior of bornite, covellite and pyrite. *Hydrometallurgy* **2009**, *95*, 104–112. [CrossRef]
50. Cortés, S.; Soto, E.E.; Ordóñez, J.I. Recovery of copper from leached tailing solutions by biosorption. *Minerals* **2020**, *10*, 158. [CrossRef]
51. Torres, C.M.; Taboada, M.E.; Graber, T.A.; Herreros, O.O.; Ghorbani, Y.; Watling, H.R. The effect of seawater based media on copper dissolution from low-grade copper ore. *Miner. Eng.* **2015**, *71*, 139–145. [CrossRef]
52. Fuentes, G.; Viñals, J.; Herreros, O. Hydrothermal purification and enrichment of Chilean copper concentrates. Part 2: The behavior of the bulk concentrates. *Hydrometallurgy* **2009**, *95*, 113–120. [CrossRef]
53. Gentina, J.C.; Acevedo, F. Application of bioleaching to copper mining in Chile. *Electron. J. Biotechnol.* **2013**, *16*, 16. [CrossRef]
54. Barkhordari, H.R.; Jorjani, E.; Eslami, A.; Noaparast, M. Occurrence mechanism of silicate and aluminosilicate minerals in Sarcheshmeh copper flotation concentrate. *Int. J. Miner. Metall. Mater.* **2009**, *16*, 494–499. [CrossRef]
55. Casas, J.M.; Crisóstomo, G.; Cifuentes, L. Antimony Solubility and Speciation in Aqueous Sulphuric Acid Solutions at 298 K. *Can. J. Chem. Eng.* **2008**, *82*, 175–183. [CrossRef]
56. Dimitrijević, M.; Kostov, A.; Tasić, V.; Milosević, N. Influence of pyrometallurgical copper production on the environment. *J. Hazard. Mater.* **2009**, *164*, 892–899. [CrossRef] [PubMed]
57. Hansen, H.K.; Yianatos, J.B.; Ottosen, L.M. Speciation and leachability of copper in mine tailings from porphyry copper mining: Influence of particle size. *Chemosphere* **2005**, *60*, 1497–1503. [CrossRef]
58. Padilla, R.; Rodríguez, G.; Ruiz, M.C. Copper and arsenic dissolution from chalcopyrite-enargite concentrate by sulfidation and pressure leaching in H_2SO_4-O_2. *Hydrometallurgy* **2010**, *100*, 152–156. [CrossRef]
59. Cruz, C.; Reyes, A.; Jeldres, R.I.; Cisternas, L.A.; Kraslawski, A. Using Partial Desalination Treatment to Improve the Recovery of Copper and Molybdenum Minerals in the Chilean Mining Industry. *Ind. Eng. Chem. Res.* **2019**, *58*, 8915–8922. [CrossRef]
60. Araya, G.; Toro, N.; Castillo, J.; Guzmán, D.; Guzmán, A.; Hernández, P.; Jeldres, R.I.; Sepúlveda, R. Leaching of oxide copper ores by addition of weak acid from copper smelters. *Metals* **2020**, *10*, 627. [CrossRef]
61. Voisin, L. New Strategies for the Treatment of Copper Concentrates with High Arsenic Content in Chile. Available online: http://mric.jogmec.go.jp/public/kouenkai/2012-11/briefing_121108_5new.pdf (accessed on 20 December 2021).
62. Yianatos, J.; Vallejos, P.; Grau, R.; Yañez, A. New approach for flotation process modelling and simulation. *Miner. Eng.* **2020**, *156*, 106482. [CrossRef]
63. Mathe, E.; Cruz, C.; Lucay, F.A.; Gálvez, E.D.; Cisternas, L.A. Development of a grinding model based on flotation performance. *Miner. Eng.* **2021**, *166*, 106890. [CrossRef]
64. Deng, J.; Wen, S.; Xian, Y.; Bai, S.; Liu, D.; Shen, H. Efficient utilization of copper sulfide ore in Chile by flotation. *Adv. Mater. Res.* **2012**, *524–527*, 975–982. [CrossRef]

65. Palencia, I.; Romero, R.; Mazuelos, A.; Carranza, F. Treatment of secondary copper sulphides (chalcocite and covellite) by the BRISA process. *Hydrometallurgy* **2002**, *66*, 85–93. [CrossRef]
66. Vallejos, P.; Yianatos, J. Analysis of Industrial Flotation Circuits Using Top-of-froth and Concentrate Mineralogy. *Miner. Process. Extr. Metall. Rev.* **2021**, *42*, 511–520. [CrossRef]
67. Ballantyne, G.R.; Powell, M.S. Benchmarking comminution energy consumption for the processing of copper and gold ores. *Miner. Eng.* **2014**, *65*, 109–114. [CrossRef]
68. Ekrem Yüce, A.; Mustafa Tarkan, H.; Zeki Doğan, M. Effect of bacterial conditioning and the flotation of copper ore and concentrate. *Afr. J. Biotechnol.* **2006**, *5*, 448–452.
69. Larouche, P. Minor Elements in Copper Smelting and Electrorefining. Master's Thesis, McGill University, Montréal, QC, Canada, 2001.
70. Senior, G.D.; Guy, P.J.; Bruckard, W.J. The selective flotation of enargite from other copper minerals—A single mineral study in relation to beneficiation of the Tampakan deposit in the Philippines. *Int. J. Miner. Process.* **2006**, *81*, 15–26. [CrossRef]
71. Smith, L.K.; Bruckard, W.J. The separation of arsenic from copper in a Northparkes copper-gold ore using controlled-potential flotation. *Int. J. Miner. Process.* **2007**, *84*, 15–24. [CrossRef]
72. Finch, J.A.; Tan, Y.H. A comparison of two flotation circuits. *Miner. Eng.* **2021**, *170*, 107002. [CrossRef]
73. Cisternas, L.A.; Lucay, F.A.; Acosta-Flores, R.; Gálvez, E.D. A quasi-review of conceptual flotation design methods based on computational optimization. *Miner. Eng.* **2018**, *117*, 24–33. [CrossRef]
74. Jamett, N.; Cisternas, L.; Vielma, J.P. *Solution Strategies to Stochastic Design of Mineral Flotation Plants*; Elsevier: Amsterdam, The Netherlands, 2014; Volume 34.
75. Hassanzadeh, A.; Hasanzadeh, M. Chalcopyrite and pyrite floatabilities in the presence of sodium sulfide and sodium metabisulfite in a high pyritic copper complex ore. *J. Dispers. Sci. Technol.* **2017**, *38*, 782–788. [CrossRef]
76. Lü, C.; Wang, Y.; Qian, P.; Liu, Y.; Fu, G.; Ding, J.; Ye, S.; Chen, Y. Separation of chalcopyrite and pyrite from a copper tailing by ammonium humate. *Chin. J. Chem. Eng.* **2018**, *26*, 1814–1821. [CrossRef]
77. Flores, G.A.; Risopatron, C.; Pease, J. Processing of Complex Materials in the Copper Industry: Challenges and Opportunities Ahead. *JOM* **2020**, *72*, 3447–3461. [CrossRef] [PubMed]
78. Moreno, P.A.; Aral, H.; Cuevas, J.; Monardes, A.; Adaro, M.; Norgate, T.; Bruckard, W. The use of seawater as process water at Las Luces copper-molybdenum beneficiation plant in Taltal (Chile). *Miner. Eng.* **2011**, *24*, 852–858. [CrossRef]
79. Cisternas, L.A.; Gálvez, E.D. The use of seawater in mining. *Miner. Process. Extr. Metall. Rev.* **2018**, *39*, 18–33. [CrossRef]
80. Sernageomin. *Catastro de Depósitos de Relaves en Chile*; Sernageomin: Santiago, Chile, 2020. Available online: https://www.sernageomin.cl/datos-publicos-deposito-de-relaves/ (accessed on 20 December 2021).
81. Lyu, Z.; Chai, J.; Xu, Z.; Qin, Y.; Cao, J. A Comprehensive Review on Reasons for Tailings Dam Failures Based on Case History. *Adv. Civ. Eng.* **2019**, *2019*, 4159306. [CrossRef]
82. Hesketh, A.H.; Broadhurst, J.L.; Harrison, S.T.L. Mitigating the generation of acid mine drainage from copper sulfide tailings impoundments in perpetuity: A case study for an integrated management strategy. *Miner. Eng.* **2010**, *23*, 225–229. [CrossRef]
83. Demetrio, S.; Ahumada, J.; Duran, M.A.; Mast, E.; Rojas, U.; Sanhueza, J.; Reyes, P.; Morales, E. Slag cleaning: The Chilean copper smelter experience. *JOM* **2000**, *52*, 20–25. [CrossRef]
84. Huisman, J.L.; Schouten, G.; Schultz, C. Biologically produced sulphide for purification of process streams, effluent treatment and recovery of metals in the metal and mining industry. *Hydrometallurgy* **2006**, *83*, 106–113. [CrossRef]
85. Smuda, J.; Dold, B.; Spangenberg, J.E.; Friese, K.; Kobek, M.R.; Bustos, C.A.; Pfeifer, H.R. Element cycling during the transition from alkaline to acidic environment in an active porphyry copper tailings impoundment, Chuquicamata, Chile. *J. Geochem. Explor.* **2014**, *140*, 23–40. [CrossRef]
86. Vargas, F.; Lopez, M.; Rigamonti, L. Environmental impacts evaluation of treated copper tailings as supplementary cementitious materials. *Resour. Conserv. Recycl.* **2020**, *160*, 104890. [CrossRef]
87. Vargas, F.; Alsina, M.A.; Gaillard, J.F.; Pasten, P.; Lopez, M. Copper entrapment and immobilization during cement hydration in concrete mixtures containing copper tailings. *J. Clean. Prod.* **2021**, *312*, 127547. [CrossRef]
88. Marín, O.; Valderrama, J.O.; Kraslawski, A.; Cisternas, L.A. Potential of tailing deposits in chile for the sequestration of carbon dioxide produced by power plants using ex-situ mineral carbonation. *Minerals* **2021**, *11*, 320. [CrossRef]
89. Araya, N.; Ramírez, Y.; Kraslawski, A.; Cisternas, L.A. Feasibility of re-processing mine tailings to obtain critical raw materials using real options analysis. *J. Environ. Manag.* **2021**, *284*, 112060. [CrossRef] [PubMed]
90. Araya, N.; Kraslawski, A.; Cisternas, L.A. Towards mine tailings valorization: Recovery of critical materials from Chilean mine tailings. *J. Clean. Prod.* **2020**, *263*, 121555. [CrossRef]
91. Imris, I.; Rebolledo, S.; Sanchez, M.; Castro, G.; Achurra, G.; Hernandez, F. The Copper Losses in the Slags From the El Teniente Process. *Can. Metall. Q.* **2000**, *39*, 281–290. [CrossRef]
92. Lam, E.J.; Gálvez, M.E.; Cánovas, M.; Montofré, I.L.; Rivero, D.; Faz, A. Evaluation of metal mobility from copper mine tailings in northern Chile. *Environ. Sci. Pollut. Res.* **2016**, *23*, 11901–11915. [CrossRef]
93. Medina Tripodi, E.E.; Gamboa Rueda, J.A.; Aguirre Céspedes, C.; Delgado Vega, J.; Collao Gómez, C. Characterization and geostatistical modelling of contaminants and added value metals from an abandoned Cu–Au tailing dam in Taltal (Chile). *J. South Am. Earth Sci.* **2019**, *93*, 183–202. [CrossRef]

94. Santibáñez, C.; Verdugo, C.; Ginocchio, R. Phytostabilization of copper mine tailings with biosolids: Implications for metal uptake and productivity of Lolium perenne. *Sci. Total Environ.* **2008**, *395*, 1–10. [CrossRef]
95. Villarroel, D. Process for refining copper in solid state. *Miner. Eng.* **1999**, *12*, 405–414. [CrossRef]
96. Cifuentes, G.; Simpson, J.; Zúñiga, C.; Briones, L.; Morales, A. Model and simulation of an ion exchange process for the extraction of antimony. *J. Metall. Eng.* **2012**, *1*, 75–85.
97. Toro, N.; Ayala, L.; Pérez, K.; Castillo, J.; Navarra, A. Economic and strategic analysis of the current situation of Chilean copper smelters. In Proceedings of the AIP Conference Proceedings, Indore, India, 14–16 December 2020; Volume 2281, p. 020008.
98. Imris, I.; Sánchez, M.; Achurra, G. Copper losses to slags obtained from the El Teniente process. *Trans. Inst. Min. Metall. Sect. C Miner. Process. Extr. Metall.* **2005**, *114*, 135–140. [CrossRef]
99. Bengoa, J.; Palacios, J.; Sánchez, M. Effect of oxygen enrichment in El Teniente Converter productivity at the Ilo Smelter Plant, Peru. In Proceedings of the TMS Yazawa International Symposium on Metallurgical Thermochemistry and Materials Processing, San Diego, CA, USA, 2–6 March 2003.
100. Goñi, C.; Sanchez, M. Modelling of copper content variation during "El Teniente" slag cleaning process. In Proceedings of the VIII International Conference Molten 2009, Santiago, Chile, 18–21 January 2009; pp. 1203–1210.
101. Artzer, A.; Moats, M.; Bender, J. Removal of Antimony and Bismuth from Copper Electrorefining Electrolyte: Part I—A Review. *JOM* **2018**, *70*, 2033–2040. [CrossRef]
102. Chen, T.T.; Dutrizac, J.E. Mineralogical characterization of anode slimes: Part 7—Copper anodes and anode slimes from the chuquicamat a division of codelco-Chile. *Can. Metall. Q.* **1991**, *30*, 95–106. [CrossRef]
103. Cifuentes, G.; Vargas, C.; Simpson, J. Analisis de las principales variables de proceso que influyen en el rechazo de los cátodos durante el electrorrefino del cobre. *Rev. Metal.* **2009**, *45*, 228–236. [CrossRef]
104. Cifuentes, G.; Hernández, S.; Navarro, P.; Simpson, J.; Reyes, C.; Naranjo, A.; Tapia, L. Anodic Slimes Characteristics and Behaviour in Copper Refining. In Proceedings of the Copper, Phoenix, AZ, USA, 10–13 October 1999; pp. 427–435.
105. Roy, S.; Sarkar, S.; Datta, A.; Rehani, S. Importance of mineralogy and reaction kinetics for selecting leaching methods of copper from copper smelter slag. *Sep. Sci. Technol.* **2016**, *51*, 135–146. [CrossRef]
106. Zhou, H.; Liu, G.; Zhang, L.; Zhou, C. Mineralogical and morphological factors affecting the separation of copper and arsenic in flash copper smelting slag flotation beneficiation process. *J. Hazard. Mater.* **2021**, *401*, 123293. [CrossRef]
107. Busolic, D.; Parada, F.; Parra, R.; Sanchez, M.; Palacios, J.; Hino, M. Recovery of iron from copper flash smelting slags. *Trans. Inst. Min. Metall. Sect. C Miner. Process. Extr. Metall.* **2011**, *120*, 32–36. [CrossRef]
108. Cardona, N.; Coursol, P.; MacKey, P.J.; Parra, R.; Vargas, J.; Parra, R. The physical chemistry of copper smelting slags and copper losses at the Paipote smelter part 2—Characterisation of industrial slags. *Can. Metall. Q.* **2011**, *50*, 330–340. [CrossRef]
109. Herreros, O.; Quiroz, R.; Manzano, E.; Bou, C.; Viñals, J. Copper extraction from reverberatory and flash furnace slags by chlorine leaching. *Hydrometallurgy* **1998**, *49*, 87–101. [CrossRef]
110. Nazer, A.S.; Pavez, O.; Rojas, F. Use of copper slag in cement mortar. *Rem Rev. Esc. Minas* **2012**, *65*, 87–91. [CrossRef]
111. Yang, Z.; Rui-Lin, M.; Wang-Dong, N.; Hui, W. Selective leaching of base metals from copper smelter slag. *Hydrometallurgy* **2010**, *103*, 25–29. [CrossRef]
112. Banza, A.N.; Gock, E.; Kongolo, K. Base metals recovery from copper smelter slag by oxidising leaching and solvent extraction. *Hydrometallurgy* **2002**, *67*, 63–69. [CrossRef]
113. Li, Y.; Papangelakis, V.G.; Perederiy, I. High pressure oxidative acid leaching of nickel smelter slag: Characterization of feed and residue. *Hydrometallurgy* **2009**, *97*, 185–193. [CrossRef]
114. Li, Y.; Perederiy, I.; Papangelakis, V.G. Cleaning of waste smelter slags and recovery of valuable metals by pressure oxidative leaching. *J. Hazard. Mater.* **2008**, *152*, 607–615. [CrossRef] [PubMed]
115. Baghalha, M.; Papangelakis, V.G.; Curlook, W. Factors affecting the leachability of Ni/Co/Cu slags at high temperature. *Hydrometallurgy* **2007**, *85*, 42–52. [CrossRef]
116. Sánchez, M.; Sudbury, M. Physicochemical characterization of copper slag and alternatives of friendly environmental management. *J. Min. Metall. Sect. B Metall.* **2013**, *49*, 161–168. [CrossRef]
117. Parada, F.; Parra, R.; Marquez, F.; Jara, R.; Carrasco, J.C.; Palacios, J. Management of copper pyrometallurgical slags: Giving additional value to copper mining industry. In Proceedings of the VII International Conference on Molten Slags, Fluxes & Salts, Cape Town, South Africa, 25–28 January 2004; pp. 543–550.
118. Chen, Y.; Liao, T.; Li, G.; Chen, B.; Shi, X. Recovery of bismuth and arsenic from copper smelter flue dusts after copper and zinc extraction. *Miner. Eng.* **2012**, *39*, 23–28. [CrossRef]
119. Balladares, E.; Kelm, U.; Helle, S.; Parra, R.; Araneda, E. Chemical-mineralogical characterization of copper smelting flue dust. *DYNA* **2014**, *81*, 11–18. [CrossRef]
120. Berasaluce, M.; Mondaca, P.; Schuhmacher, M.; Bravo, M.; Sauvé, S.; Navarro-Villarroel, C.; Dovletyarova, E.A.; Neaman, A. Soil and indoor dust as environmental media of human exposure to As, Cd, Cu, and Pb near a copper smelter in central Chile. *J. Trace Elem. Med. Biol.* **2019**, *54*, 156–162. [CrossRef]
121. Gonzalez-Montero, P.; Iglesias-Gonzalez, N.; Romero, R.; Mazuelos, A.; Carranza, F. Recovery of zinc and copper from copper smelter flue dust. Optimisation of sulphuric acid leaching. *Environ. Technol.* **2020**, *41*, 1093–1100. [CrossRef]
122. Okanigbe, D.O.; Popoola, A.P.I.; Adeleke, A.A. Characterization of Copper Smelter Dust for Copper Recovery. *Procedia Manuf.* **2017**, *7*, 121–126. [CrossRef]

123. Alguacil, F.J.; Garcia-Diaz, I.; Lopez, F.; Rodriguez, O. Recycling of copper flue dust via leaching-solvent extraction processing. *Desalin. Water Treat.* **2015**, *56*, 1202–1207. [CrossRef]
124. González, A.; Font, O.; Moreno, N.; Querol, X.; Arancibia, N.; Navia, R. Copper Flash Smelting Flue Dust as a Source of Germanium. *Waste Biomass Valorization* **2017**, *8*, 2121–2129. [CrossRef]
125. Cifuentes, G.; Hernández, J.; Guajardo, N. Recovering Scrap Anode Copper Using Reactive Electrodialysis. *Am. J. Anal. Chem.* **2014**, *05*, 1020–1027. [CrossRef]
126. Ilkhchi, M.O.; Yoozbashizadeh, H.; Safarzadeh, M.S. The effect of additives on anode passivation in electrorefining of copper. *Chem. Eng. Process. Process Intensif.* **2007**, *46*, 757–763. [CrossRef]
127. Acharya, S. Copper refining electrolyte and slime processing—Emerging techniques. *Adv. Mater. Res.* **2014**, *828*, 93–115. [CrossRef]
128. Loira, P.S.; Mikenberg, D.C. Reusable Anode System for Electrorefining Processes. U.S. Patent Application 14/768,022, 3 March 2016.
129. Cifuentes, G.; Hernández, J.; Manríquez, J.; Guajardo, N. Modeling Operational Parameters of a Reactive Electro-Dialysis Cell for Electro-Refining Anodic Scrap Copper. *Am. J. Anal. Chem.* **2014**, *5*, 1011–1019. [CrossRef]
130. Zeng, W.; Free, M.L.; Wang, S. Studies of Anode Slime Sintering/Coalescence and Its Effects on Anode Slime Adhesion and Cathode Purity in Copper Electrorefining. *J. Electrochem. Soc.* **2016**, *163*, E14–E31. [CrossRef]
131. Hiskey, J.B.; Moats, M.S. Periodic oscillations during electrolytic dissolution of copper anodes. In Proceedings of the Copper, Electrowinning and Refining, Clausthal-Zellerfeld, Germany, 6–10 June 2010; Volume 4, pp. 1367–1377.
132. Hoffmann, J.E. The Purification of Copper Refinery Electrolyte. *JOM* **2004**, *56*, 30–33. [CrossRef]
133. Liu, G.; Wu, Y.; Tang, A.; Pan, D.; Li, B. Recovery of scattered and precious metals from copper anode slime by hydrometallurgy: A review. *Hydrometallurgy* **2020**, *197*, 105460. [CrossRef]
134. Hait, J.; Jana, R.K.; Sanyal, S.K. Processing of copper electrorefining anode slime: A review. *Miner. Process. Extr. Metall.* **2009**, *118*, 240–252. [CrossRef]
135. Xing, W.D.; Sohn, S.H.; Lee, M.S. A Review on the Recovery of Noble Metals from Anode Slimes. *Miner. Process. Extr. Metall. Rev.* **2020**, *41*, 130–143. [CrossRef]
136. Moats, M.; Robinson, T.; Davenport, W.; Karcas, G.; Demetrio, S. Electrolytic copper refining—2007 world tankhouse operating data. In *Copper Electrorefining and Electrowinning*; Canadian Institute of Mining: Montreal, QC, Canada, 2007; pp. 195–241.
137. Moats, M.S.; Hiskey, J.B. Role of electrolyte additives on passivation behaviour during copper electrorefining. *Can. Metall. Q.* **2000**, *39*, 297–306. [CrossRef]
138. Cifuentes, G.; Guajardo, N.; Hernández, J. Recovery of hydrochloric acid from ion exchange processes by reactive electrodialysis. *J. Chil. Chem. Soc.* **2015**, *60*, 2711–2715. [CrossRef]
139. Petkova, E.N. Mechanisms of floating slime formation and its removal with the help of sulphur dioxide during the electrorefining of anode copper. *Hydrometallurgy* **1997**, *46*, 277–286. [CrossRef]
140. Vikström, H. Is There a Supply Crisis? Sweden's Critical Metals, 1917–2014. *Extr. Ind. Soc.* **2018**, *5*, 393–403. [CrossRef]
141. Anderson, C.G. The metallurgy of antimony. *Geochemistry* **2012**, *72*, 3–8. [CrossRef]
142. Filella, M.; Belzile, N.; Chen, Y.W. Antimony in the environment: A review focused on natural waters I. Occurence. *Earth-Sci. Rev.* **2002**, *57*, 125–176. [CrossRef]
143. Hočevar, S.B.; Ogorevc, B.; Wang, J.; Pihlar, B. A study on operational parameters for advanced use of bismuth film electrode in anodic stripping voltammetry. *Electroanalysis* **2002**, *14*, 1707–1712. [CrossRef]
144. Sverdrup, H.U.; Ragnarsdottir, K.V.; Koca, D. An assessment of metal supply sustainability as an input to policy: Security of supply extraction rates, stocks-in-use, recycling, and risk of scarcity. *J. Clean. Prod.* **2017**, *140*, 359–372. [CrossRef]
145. Müller, S.; Schötz, C.; Picht, O.; Sigle, W.; Kopold, P.; Rauber, M.; Alber, I.; Neumann, R.; Toimil-Molares, M.E. Electrochemical synthesis of Bi 1-xSb x nanowires with simultaneous control on size, composition, and surface roughness. *Cryst. Growth Des.* **2012**, *12*, 615–621. [CrossRef]
146. Shabani, A.; Hoseinpur, A.; Yoozbashizadeh, H.; Vahdati Khaki, J. As, Sb, and Fe removal from industrial copper electrolyte by solvent displacement crystallisation technique. *Can. Metall. Q.* **2019**, *58*, 253–261. [CrossRef]
147. Zeraati, M.; Chauhan, N.P.S.; Sargazi, G. Removal of electrolyte impurities from industrial electrolyte of electro-refining copper using green crystallization approach. *Chem. Pap.* **2021**, *75*, 3873–3880. [CrossRef]
148. Cifuentes, G.A.; Simpson, J.R.; Vargas, C.A. Precipitation of Antimony and Bismuth from Copper Refinery Electrolyte Using PbO_2. U.S. Patent Application 13/917,342, 17 October 2013.
149. Cifuentes, M.; Cifuentes, G.; Simpson, J.; Zúñiga, C. A comparative study of ion exchange process for the extraction of antimony. In Proceedings of the Copper 2013, Santiago, Chile, 8–10 April 2013.
150. Riveros, P.A.; Dutrizac, J.E.; Lastra, R. A study of the ion exchange removal of antimony(III) and antimony(V) from copper electrolytes. *Can. Metall. Q.* **2008**, *47*, 307–316. [CrossRef]
151. McKevitt, B.; Dreisinger, D. A comparison of various ion exchange resins for the removal of ferric ions from copper electrowinning electrolyte solutions Part II: Electrolytes containing antimony and bismuth. *Hydrometallurgy* **2009**, *98*, 122–127. [CrossRef]
152. Ruiz, I.; Rios, G.; Arbizu, C.; Hanschke, U.; Burke, I. Pilot tests on bismuth and antimony removal from electrolyte at atlantic copper refinery. In Proceedings of the European Metallurgical Conference (EMC), Weimar, Germany, 23–26 June 2013; pp. 85–98.
153. Ando, K.; Tsuchida, N. Recovering Bi and Sb from electrolyte in copper electrorefining. *JOM* **1997**, *49*, 49–51. [CrossRef]

154. Moghimi, F.; Jafari, A.H.; Yoozbashizadeh, H.; Askari, M. Adsorption behavior of Sb(III) in single and binary Sb(III)—Fe(II) systems on cationic ion exchange resin: Adsorption equilibrium, kinetic and thermodynamic aspects. *Trans. Nonferrous Met. Soc. China* **2020**, *30*, 236–248. [CrossRef]
155. Nagai, T. Purification of copper electrolyte by solvent extraction and ion-exchange techniques. *Miner. Process. Extr. Metall. Rev.* **1997**, *17*, 143–168. [CrossRef]
156. Riveros, P.A. Method to Remove Antimony from Copper Electrolytes. U.S. Patent 8,349,187, 8 January 2013.
157. Kryst, K.; Simmons, P. Antimony and Bismuth Control in Copper Electrolyte by Ion Exchange. In *Extraction*; Springer International Publishing: Cham, Switzerland, 2018; pp. 2107–2111. ISBN 978-3-319-95021-1.